Indigenous and contaminant microbes in ultradeep mines

T. C. Onstott,[1]* D. P. Moser,[2] S. M. Pfiffner,[3]
J. K. Fredrickson,[2] F. J. Brockman,[2] T. J. Phelps,[4]
D. C. White,[3] A. Peacock,[3] D. Balkwill,[5] R. Hoover,[6]
L. R. Krumholz,[7] M. Borscik,[1] T. L. Kieft[8] and R. Wilson[9]

[1]*Department of Geosciences, Princeton University, Princeton, NJ 08544, USA.*
[2]*Pacific Northwest National Laboratory, 902 Battelle Blvd., Mail Stop P7-50, PO Box 999, Richland, WA 99352, USA.*
[3]*Department of Microbiology, The University of Tennessee, Center for Biomarker Analysis, 10515 Research Dr., Ste. 300, Knoxville, TN 37932–2575, USA.*
[4]*Environmental Sciences Division, Oak Ridge National Laboratory, PO Box 2008, Oak Ridge, TN 37831–6036, USA.*
[5]*Department of Biological Science, Florida State University, 312 NRB, B-162, Tallahassee, FL 32306, USA.*
[6]*George Marshall Space Flight Center/NASA, SD-50, Huntsville, AL 35812, USA.*
[7]*Department of Botany and Microbiology, University of Oklahoma, 770 Van Vleet Oval, Norman, OK 73019, USA.*
[8]*Department of Biology, 801 Leroy St, New Mexico Institute of Mining and Technology, Socorro, NM 87801, USA.*
[9]*SRK-Turgis Technology, 299 Pendoring St, Blackheath, 2115 South Africa.*

Summary

Rock, air and service water samples were collected for microbial analyses from 3.2 kilometres depth in a working Au mine in the Witwatersrand basin, South Africa. The ~ metre-wide mined zone was comprised of a carbonaceous, quartz, sulphide, uraninite and Au bearing layer, called the Carbon Leader, sandwiched by quartzite and conglomerate. The microbial community in the service water was dominated by mesophilic aerobic and anaerobic, α-, β- and γ-*Proteobacteria* with a total biomass concentration ~10^4 cells ml^{-1}, whereas, that of the mine air was dominated by members of the *Chlorobi* and *Bacteroidetes* groups and a fungal component. The microorganisms in the Carbon Leader were predominantly mesophilic, aerobic heterotrophic, nitrate reducing and methylotrophic, β- and γ-*Proteobacteria* that were more closely related to service water microorganisms than to air microbes. Rhodamine WT dye and fluorescent microspheres employed as contaminant tracers, however, indicated that service water contamination of most of the rock samples was <0.01% during acquisition. The microbial contaminants most likely originated from the service water, infiltrated the low permeability rock through and accumulated within mining-induced fractures where they survived for several days before being mined. Combined PLFA and terminal restriction fragment length profile (T-RFLP) analyses suggest that the maximum concentration of indigenous microorganisms in the Carbon Leader was <10^2 cells g^{-1}. PLFA, ^{35}S autoradiography and enrichments suggest that the adjacent quartzite was less contaminated and contained ~10^3 cells $gram^{-1}$ of thermophilic, sulphate reducing bacteria, SRB, some of which are δ-*Proteobacteria*. Pore water and rock geochemical analyses suggest that these SRB's may have been sustained by sulphate diffusing from the adjacent U-rich, Carbon Leader where it was formed by radiolysis of sulphide.**

Introduction

The nature of the microbial biomass distribution and microbial community structure in the deep subsurface and the factors that control it, remain largely unknown (Onstott *et al.*, 1998a). Because water at great depths is confined to fractures, microorganisms are expected to be concentrated along the fracture surfaces and to diminish in abundance with increasing distance from the fracture towards the interior matrix of the rock strata. Presumably, geochemical heterogeneity also influences the biomass distribution as it does in relatively shallow environments with much of the biomass localized along interfaces where the electron donor and acceptor flux is higher than within homogenous layers (Krumholz *et al.*, 1997). The porosity and permeability also influence this flux and the movement of microorganisms (Fredrickson *et al.*, 1997). Only a few cores from depths >1 kilometre below land surface (kmbls) have been characterized with regard to their microbiological properties. A sidewall, shale core from 2.7 kmbls in the Taylorsville Basin of eastern Virginia contained 16 pmole g^{-1} of prokaryotic PLFA (Onstott *et al.*, 1998b) roughly equivalent to 4×10^5 bacterial cells g^{-1}

(White and Ringelberg, 1998), whereas, a sandstone core collected from 2.0 kmbls in the Piceance Basin of western Colorado contained only 0.4 pmole g^{-1} (Colwell *et al.*, 1997) or 1×10^4 bacterial cells g^{-1}. In both cases, tracers were utilized to identify potential contamination from drilling mud and precautions were taken to reduce contamination during processing. The differences in biomass between these two samples may be related to their distinct thermal histories. The sample from the Piceance Basin cooled below 120°C within the last 5 Myr. (Colwell *et al.*, 2002), whereas, the Taylorsville Basin sample cooled below 120°C, 160 Myr ago (Tseng *et al.*, 1995). It is impossible to draw inferences about the subsurface biosphere based upon just two samples collected from such disparate locations. These studies nevertheless illustrate the complexities encountered when investigating the presence and function of microorganisms deep within the earth's crust.

To determine the relationships between microbial properties and the chemical and physical heterogeneity of a crustal section requires at the least: (i) ready access to a variety of rock types across a range of spatial scales from centimetres to hundreds of metres and down to depths of kilometres, and (ii) an environment for which the ambient temperature has remained constant for a geologically significant period of time. The deep Au mines of the Witwatersrand basin in South Africa fulfill both criteria. Mining in the Witwatersrand basin occurs along several different horizons, some in a conglomerate unit containing thin organic layers within the Central Rand Group and another in the contact between quartzite of the Central Rand Group and the overlying Ventersdorp volcanic rock. The contacts can be sampled at varying distances from crosscutting water and gas bearing dykes and fractures. The organic carbon and U content of the Au-bearing seams ranges up to 34 and 10 wt.% respectively (Zumberge *et al.*, 1978; Gray *et al.*, 1998). The radiolysis of pore water caused by the high concentration of U produces molecular H_2, O_2 and H_2O_2 (Hoffman, 1992) providing a potential energy source for microorganisms. Analyses of fission tracks in apatites indicate that the paleotemperature has been constant for the past 30 Myr and slowly cooled at ~ 1°C my^{-1} from 80 to 30 Ma (Omar *et al.*, 2003). Noble gas isotopic analyses of the saline formation water at ~3 kmbls have yielded subsurface residence times ranging from 77 to 170 Ma (Lippmann *et al.*, 2003). This constrains the maximum habitability time to ~80 Ma for this depth (Omar *et al.*, 2003).

Carbon Leader samples from a 3.23 kmbls freshly mined face at Mponeng Au mine near Carletonville, South Africa contained 0.3–62 pmole of PLFA or the equivalent of 10^4–10^6 cells g^{-1} (Onstott *et al.*, 1997). Because PLFA is not expected to survive for billions of years (White *et al.*, 1979), Onstott *et al.* (1997) speculated that the PLFA denoted 'living', though not necessarily active, microbial communities in the deep ore zones of South Africa. Although Onstott *et al.* (1997) minimized contamination during sample processing, contamination during mining could not be precluded and the origin of these microbial signatures therefore was uncertain.

Characterizing microbial mining contamination of rock samples in an ultradeep mine is especially challenging, because the two principal contaminant sources are the ~10^6 L day^{-1} of chilled water and ~10^9 L day^{-1} of air that are circulating underground. Air is drawn down from surface through vertical and subvertical shafts, passed through the workings and back up separate shafts by surface fans (Fig. 1). As air descends into the mine, its temperature increases ~6°C per 1000 m of vertical drop. The temperature for optimal human mining is <27°C, which is attained at 1.5 kmbls. To mine at greater depths, the air must be cooled underground by industrial-scale air chillers that use water that has in turn been cooled by large surface or underground refrigeration units and then piped to the air chillers. This cooling water, referred to as service water, is also used as a drilling lubricant and is sprayed on the stope faces and floors for dust suppression.

Another problem unique to ultradeep mining is the extensive decompression fracturing caused by the extreme pressure gradients. Gay and Jager (1986) have distinguished four types of extension fractures that penetrate up to 40 m and shear fractures that penetrate up to 60 m behind the stope face (Fig. 1). Some of these fractures represent zones where service water may penetrate and remain in the mined rock face for many days before they are mined.
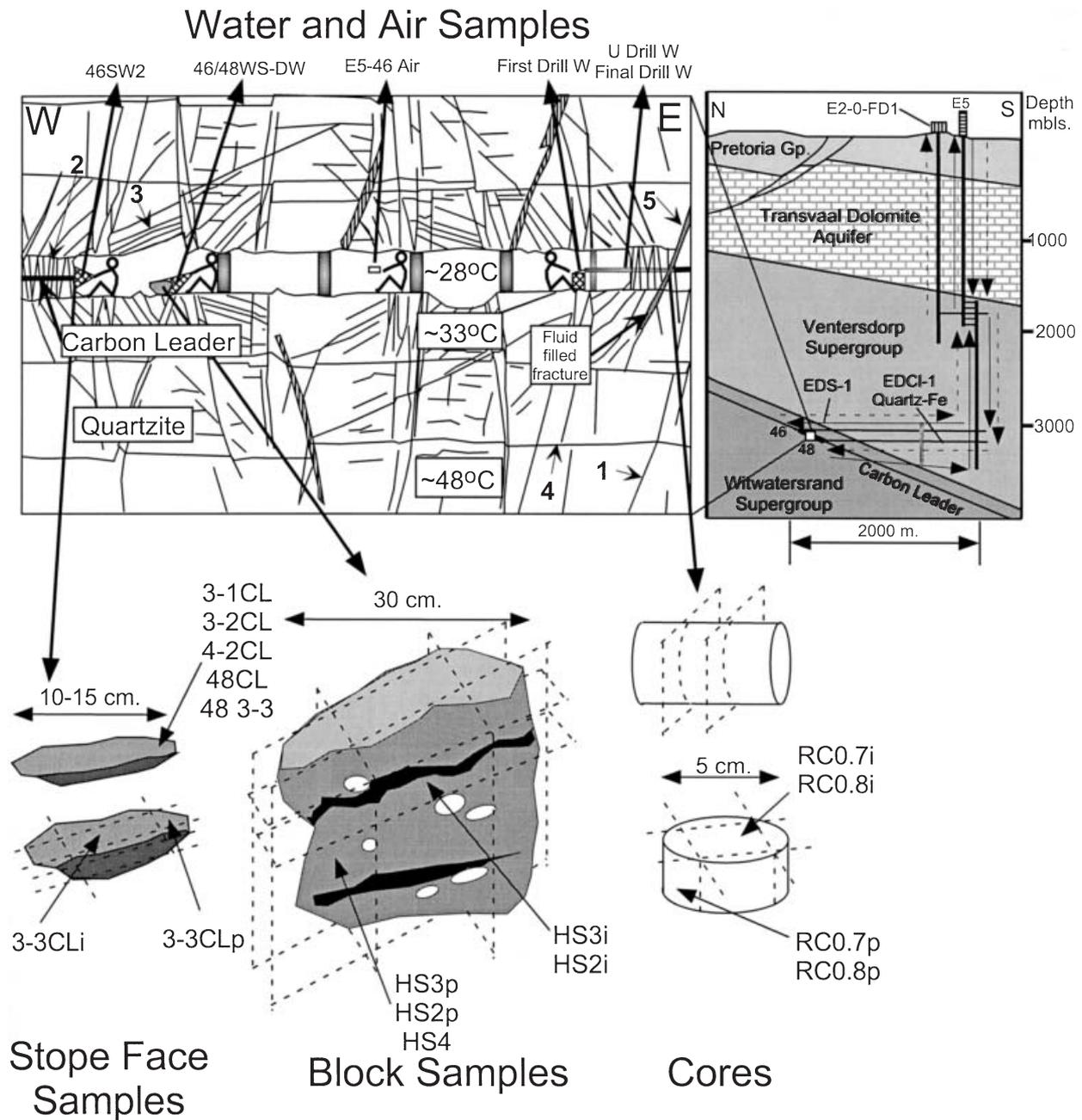
Because the service water is collected and recycled into the water circulation system and because the ventilation air traverses kilometres of tunnels before reaching the stopes, microbiota, either indigenous to the rock strata or from other sources, can become entrained within the service water and air. Tracer technology is essential to quantify the potential for contamination and to distinguish indigenous microorganisms from contaminant microbes that have been introduced from allochthonous surface and subsurface environments. Tracers used to detect and quantify contamination during drilling/coring have included solute tracers such as KBr and rhodamine dye (Phelps *et al.*, 1989) and fluorescent microspheres to track particulates such as bacteria (Colwell *et al.*, 1992). Fluorescent microspheres have been applied during sampling of rocks in mines and tunnels to trace surface contaminants in microbiological studies (Kieft *et al.*, 1997; Russell, 1997). Indigenous microbial communities in deep subsurface environments can also be distinguished from contaminant microorganisms through comparative community profiling, e.g. by PLFA analysis (Lehman *et al.*, 1995) of drilling fluids and rock samples.

In this study, we modified existing approaches to the ultradeep mining environment by applying community profiling by 16S rDNA-based molecular techniques to characterize microbial contaminants and constituents of the rocks, of the ventilation air, of the water used in removing the rocks from the stopes and of the water present in the mining-induced fractures. From these results optimal approaches for minimizing contamination and for accurately measuring the indigenous microbial biomass and composition of deep mine samples have been devised.

No. 5 Shaft East of the Driefontein Consolidated Mine, located ∼70 km west of Johannesburg, was chosen for this study, because it was among the newest of the area's ultradeep excavations, was 2 km from other mines and was extracting only the Carbon Leader horizon, leaving the shallower depths unimpacted by mining operations. The rock samples were collected at 3.25 kmbls. in a ∼1 m high stope inclined at 30° connecting levels 46 and 48 (Fig. 1). At the time of sampling, these levels had just begun to produce ore, collateral contamination by mining operations at other levels was impossible and the ventilation air had cooled the rock face from a formation temperature of ∼48°C (Omar *et al.*, 2003) to 32–35°C (Fig. 1).

Three approaches were followed in collecting rock sam-

ples (Fig. 1): (i) samples were chiseled by hand from freshly blasted westward-facing stope faces; (ii) block samples were collected from the stope floor; and (iii) 5 cm diameter cores were collected from the eastward-facing, 2-months-old stope face after intersecting a water-filled fracture at ~0.6 m depth. Samples of the tracer amended drilling fluid were collected before and following the water intersection (Fig. 1). Hand samples were also collected from access tunnels to assess the effects of long-term exposure to their microbial community structure (Fig. 1).

Stope face samples were collected from a 10^3 cm^2 square area sprayed with bright orange paint. Rhodamine WT dye (10^6 µg l^{-1}) and fluorescent microspheres (10^6 spheres ml^{-1}) were also sprayed onto this area (~10–20 ml cm^{-2} and service water was subsequently sprayed onto the stope face to simulate how the miners use the service water following blasting to remove loose rock chips and dust, ~10–20 ml cm^{-2}. Sterilized chisels were used to loosen the samples so that they could be inserted into sterile Whirlpak bags. Of the stope face samples, 3–3CL was the most organic rich and had the greatest physical integrity (Fig. 1).

A U-rich Carbon Leader block and a U-poor quartzite block were selected using a hand-held Geiger counter (Fig. 1). The rock surfaces were sprayed with Rhodamine WT dye and fluorescent microspheres before spraying their surface with service water. The samples were then placed into a sterile autoclave bags. Block sample HS3 contained several organic rich layers (Fig. 2A) and HS4 represented an outer portion of HS3.

The cores were collected with a pneumatically powered coring tool and diamond bit. The bit was cooled with service water pumped from a 5-gallon container through the interior of the bit. This water drained from the drill hole into the stope. Rhodamine WT dye and fluorescent microspheres were added to the service water before collecting the first cores and samples of the augmented service water were collected in 50-ml sterile polypropylene tubes. Service water emanating from the drill hole during the coring was also collected in 50-ml tubes. Once the cores were removed from the coring barrel, they were sealed in plastic wrap, taped, labelled and placed inside an Ar-filled PVC tube. When the tube was filled with core, a cap was sealed to the end with apiezon grease and tape. The tube was kept approximately vertical throughout coring, loading and transport to the surface.

At the field, block, core and stope face samples were removed from their bags and PVC tubes, photographed, sprayed with a orange paint and placed inside an anaerobic glove bag (Coy Laboratory Products, Grass Lake, MI) filled with N$_2$/H$_2$ (95:5 v/v). The paint was used to mark and track particles from potentially contaminated rock surfaces during processing in the glove bag. In the glove bag the hand samples and block samples were pared into 125 cm^3 cubes and the cores were cut into 2 cm thick disks using a sterile hydraulic splitter (Fredrickson and Phelps, 1997). The outer cylindrical surfaces of the core were then pared with the hydraulic splitter leaving behind a small, 20–30 g interior fragment (Fig. 1). This fragment was preserved for PLFA analyses, but was too small for DNA analyses or for microbial enrichment experiments. Both internal fragments and external parings, in that order,

Fig. 1. Upper right – geological north–south cross section of no. 5 Shaft, East Driefontein mine. The Au bearing Carbon Leader occurs in the upper part of the 2.9 Ga Witwatersrand Supergroup. The Witwatersrand Supergroup is overlain by the volcanic units of the 2.7 Ga Ventersdorp Supergroup, which in turn is unconformably overlain by the dolomite, sediment and sills of the 2.4–2.5 Ga Transvaal Supergroup. Intrusive dykes and faults with an approximate spacing of a few hundred metres cut all of these units. Whereas the dolomite houses a significant aquifer, the Witwatersrand and Ventersdorp units at this location are generally dry. This may reflect lack of dykes and faults that cut the dolomite and provide hydraulic conduits to the deeper rock units. The Carbon Leader was first intersected at levels 46 and 48 at ~3.1–3.2 kmbls and ~2 km from the shaft. The access tunnels to the stope are shown. Service water for cooling enters and leaves the mining area through the shaft system. Service water sample EDS-1 was collected from pipe along the access tunnel at level 46. Arrows delineate the water and air circulation patterns. The service water was recycled by; (1) collection in settling ponds at the bottom of the shaft complex; (2) pumping in stages to the surface; (3) chilling to 4°C and disinfection with chlorine and bromine at the surface, and (4) returning it to the mining level along the shaft complex. The service water was piped 2 km from the shaft to the stopes and along the way some of it was used to cool the air in the tunnels. From the stopes the service water flowed along the access tunnel gutters towards settling ponds at the base of the shaft complex. Water from the overlying Transvaal dolomite was drawn from the intermediate pump chamber (IPC) to replace the service water that was lost by evaporation. Ventilation air flowed down the shafts and was guided through the access tunnels to the stopes by ventilation doors. At the time of sampling the air entered the stope at level 48 and exited at 46 level where it was drawn back up to the two-kilometre deep fan drift shaft where it was transported to the surface by fans. The fan drift is where the condensate sample, E2-0-FD1 was collected.
Upper Left (adapted after Gay and Jager, 1986) – The stopes dip 20–30°S, strike east–west and are ~1 m in height to minimize dilution of the Carbon Leader with the surrounding rock. In the stopes the service water mixed with any formation fluids intersected by mining, was heated through contact with the rocks and acquired a substantial suspension load from rock dust. The west face was being actively mined at a rate of ~0.5–1 m day^{-1} and is where the hand samples and stope face samples were collected. The east face was ~2-months-old and was cored. A fluid-filled fracture was intercepted at ~0.7 metres behind the east face. Ambient air temperature in the stope was ~28°C, but rock temperatures were ~32°C within 1 m depth and are estimated to be ~48°C at 5 m depth. Five sets of fractures are usually present around the stope (numbers with arrows). Fracture type 1 forms first, metres ahead of the stope and is generally vertical, but curves around the stope. Fracture type 2 forms after 1 and is typically ~1 metre ahead of the stope face. Fracture type 3 forms synchronously with 2 and occurs above and below the stope. Fracture type 4 develops in the bedding plane. Fracture type 5 is a mining induced shear fracture that can occur up to 60 m behind stope the face.
Bottom-locations of the three different sample types and how they were processed to produce outer parings and inner chunks are shown. Top-locations of water and air samples from stope are shown. All sample names are cited in Tables 1, 2, 4 and 5. p = external parings and i = internal chunk.
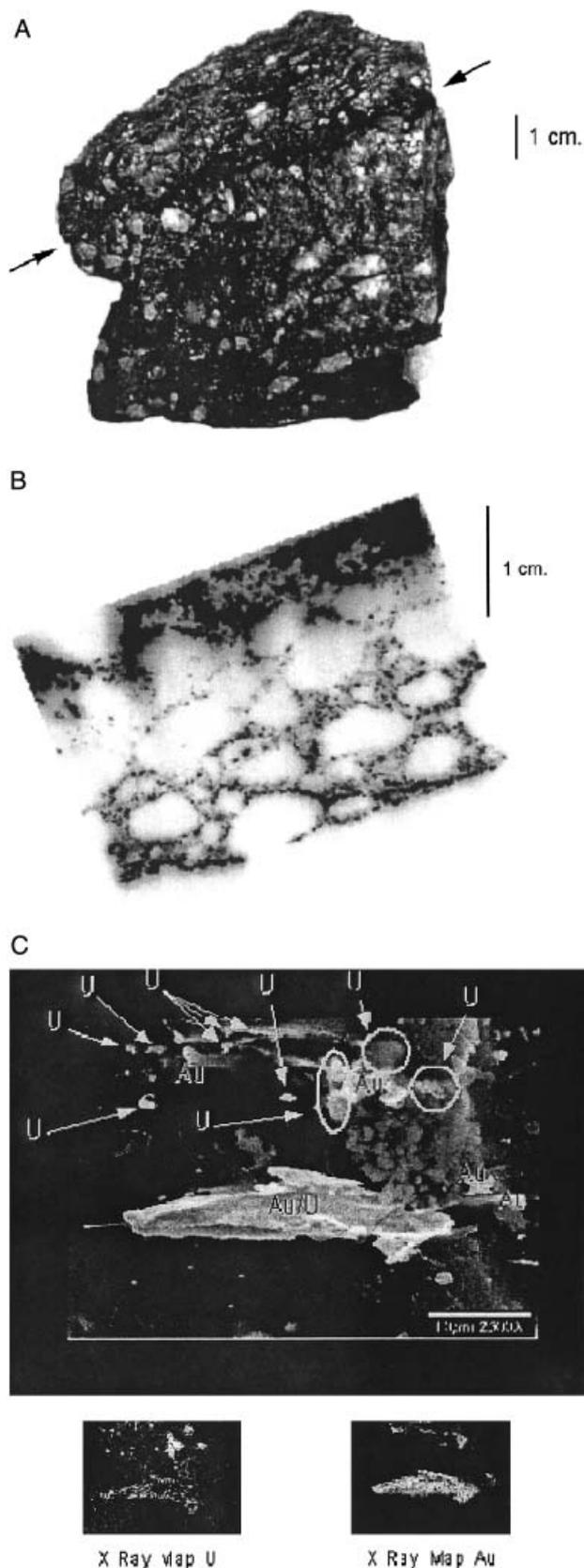
were subsequently and separately crushed with a small, sterile, stainless steel, Little Smasher, rock crusher (Rocklabs, Auckland, New Zealand). For microbial enrichments ~20–50 g of crushed rock, which varied in grain size from powder to several millimetres, was transferred with sterile spatulas into separate 140 ml sterile serum vials with 40 ml of phosphate-buffered basal mineral solution and crimp sealed. Extra pieces of the interior fragments and parings were placed in sterile Whirlpak bags, labelled, sealed in glass canning jars and frozen for DNA, petrophysical, geochemical, ^{35}S imaging and PLFA analyses. All rock processing equipment was carefully cleaned between samples to prevent cross contamination. This included washing with warm soapy water followed by a copious sterile water rinse, drying with sterilized paper towels and finally wiping down with methanol-impregnated tissue (Kim-wipes, Kimberly-Clark) to remove any traces of the rhodamine and lipids.

Service water was collected for geochemical, DNA and PLFA analyses from the hoses in the stope and from the pipeline feeding the drilling operations along the access tunnel (Fig. 1). The DNA and PLFA samples were collected using the procedure of Moser *et al.* (2003). Samples for microbial enrichments from the service water were collected in autoclaved serum vials. Particulates from a total of 4 L of air in the stope (Fig. 1) were also collected for enrichments and DNA analyses using a portable air sampler onto a membrane filter using a GilAir personal air sampler (Gilian, Redwood City, CA). Condensate from the fan drift fans at the surface was collected for PLFA analyses (Fig. 1).

Results

Tracer analyses

Of the three sample types, the internal fragments from the Carbon Leader and quartzite block samples (HS3i and HS2i in Table 1) exhibited the least degree of fracturing, lowest Rhodamine WT concentrations and no detectable fluorescent microspheres. The parings from all three sample types, e.g. HS3p, HS2p, 3-3CLp, yielded readily detectable levels of both tracers.

The initial drilling fluid tracer concentrations after it had

Fig. 2. A. Photo of Carbon Leader sample HS3, showing two carbon-rich seams and quartz pebble conglomerate. Thickness of radioactive layer is ~1 cm.
B. Phosphor image of Carbon Leader sample HS3i. Thickness of radioactive layer is 1 cm. Ovoid shaped non-radioactive zones are quartz pebbles.
C. Electron microscopic images of HS3i obtained using a Hitachi S-4000 Field Emission Scanning Electron Microscope (FESEM) with tungsten Field Emission Filament (0.5–30 kV) and Energy Dispersive Spectroscopy (EDS) Data Acquisition: Kevex Instruments located at NASA's Marshall Space Flight Center. Most of the fine-grained particles are composed of UO_2 or Au. Scale bar = 2 μm.

Table 1. Physical and chemical tracer analyses.

Sample	Microspheres (g^{-1})	Rhodamine WT (p.p.m.)	Microspheres Ts/Tc (ml g^{-1})	Rhodamine WT Ts/Tc (ml g^{-1})
spray	1000 000	1000		
Hand Samples				
HS3p	4 928	9.60	4.93E-03	9.60E-03
HS3i	<80	0.05	<8.00E-05	5.00E-05
HS2p	2 079	14.67	2.08E-03	1.47E-02
HS2i	<80	0.08	<8.00E-05	7.73E-05
HS4	N.A.	56	N.A.	5.60E-02
Stope-face samples				
3–1 CL	273 680	9.33	2.74E-01	9.33E-03
3–2 CL	147 392	16.00	1.47E-01	1.60E-02
3–3CLp	92 960	0.40	9.30E-02	4.00E-04
3–3CLi	112	<0.05	1.12E-04	<5.00E-05
Core samples				
E5 46/48 RC 0.7p	3 952	61.28	1.84E-02	9.41E-01
E5 46/48 RC 0.8p	2 192	49.71	2.18E-03	7.64E-01
Drilling water				
First Drill W	1003 440	65.1		
U Drill W	214 480	2.6	2.14E-01	3.99E-02
Final Drill W	61 956	0.52	6.17E-02	7.99E-03

Samples for microspheres were first crushed lightly to produce small chips. The crushed material was passed through a 14-mesh and 100-mesh screen to remove large chips and fines. Two ml 100 mM Na pyrophosphate and 0.25 g of the granules remaining on the 100-mesh screen were placed in a 15 ml polypropylene centrifuge tube and vortexed for 30 s. Twenty-five-µl aliquots were placed onto a glass microscope slide and covered with a 25-mm cover slip. Microspheres were counted at 200x by epifluorescence illumination with an Olympus BX60 microscope.
The samples for Rhodamine WT analysis were crushed and ground in a mortar and pestle until the material passed through a 60-mesh screen. Four ml of HPLC-grade methanol and 1.5 g of each sample were transferred to 15 ml polypropylene centrifuge tubes. The samples were then tightly sealed and shaken horizontally for 24 h at 50 r.p.m. on an orbital shaker. After extraction, the tubes were centrifuged at 2500 *g* and the liquid phase was transferred to a 5 ml syringe and filtered through 0.2 µm pore size Acrodisc syringe filters into 3 ml methacrylate spectrophotometer cuvettes. The fluorescence was measured by a fluorimeter (530 nm excitation and 555 nm emission). Samples were measured in triplicate and averaged. T_C and T_S are the measured tracer concentrations in the spray or service water, and the rock samples respectively. p refers to pairings and i refers to internal fragments.

passed through the core barrel and was leaving the drill hole were 10^6 microspheres ml^{-1} and 65 100 µg kg^{-1} of Rhodamine WT dye (First Drill W in Table 1). These concentrations decreased by 100× upon intersection of the fluid-filled fracture. Because the fracture fluid pressure was less than that of the drilling fluid, mixing with the fracture fluid occurred outside the core barrel as the drilling fluid was passing the fracture and exiting the drill hole (U Drill W and Final Drill in Table 1). Core parings yielded the highest tracer concentrations of all the rock samples (RC0.7p and 0.8p in Table 1), but their internal fragments were too small for tracer analyses.

Petrophysical and geochemical analyses

Because of the tracer results and larger sample mass, characterization focused on the Carbon Leader and quartzite block samples. Radiographic and SEM observations revealed that the pores of the Carbon Leader were filled with fine-grained sulphide, U phases (HS3i in Fig. 2B and C) and organic matter. The porosity of the Carbon Leader and the quartzite were approximately 1% and 4% respectively (Fig. 3). The permeability values calculated from the Hg porosimetry data by the approach of Swanson (1981) were below 1 µDarcy, but the 0.05 µm maxi-

mum pore throat radius of the Carbon Leader was less than that of the quartzite (Fig. 3).

The pore water chlorinity of Carbon Leader and quartzite ranged from 1450 to 2100 mg l^{-1} (HS3i and HS2i in Table 2A) and that of the crushed and leached Carbon Leader and quartzite samples was up to 21 000 mg l^{-1}. Pore water nitrate was only 0.3–4 mg l^{-1} as N but was 770–1500 mg l^{-1} in the crushed and leached extracts. Pore water sulphate ranged from 120 to 400 mg l^{-1} and was up to 11 000 mg l^{-1} in the crush and leached extracts. The principal pore water cations were Na, 500–9500 mg l^{-1}, followed by Ca, 350–4400 mg l^{-1} and Mg, 85–1010 mg l^{-1}. The pore water Fe, Mn, As and U were quite variable, with the crushed and leach extracts typically yielding the higher concentrations (Table 2A). The drilling fluid after intersection of the fluid-filled fracture yielded high nitrate concentrations (UDrill W and Final Drill in Table 2A).

Sequential extractions of the Carbon Leader and the quartzite indicated that most of the S was associated with the organic fraction and were comparable, 0.8–1.0 wt.% and 0.5–0.6 wt.% respectively (Table 2B). Sulphide was the second greatest reservoir of S. In both rock types, most of the Fe and Mn was associated with the dithionite-reducible, Fe(III) oxide or oxyhydroxide phases. The U
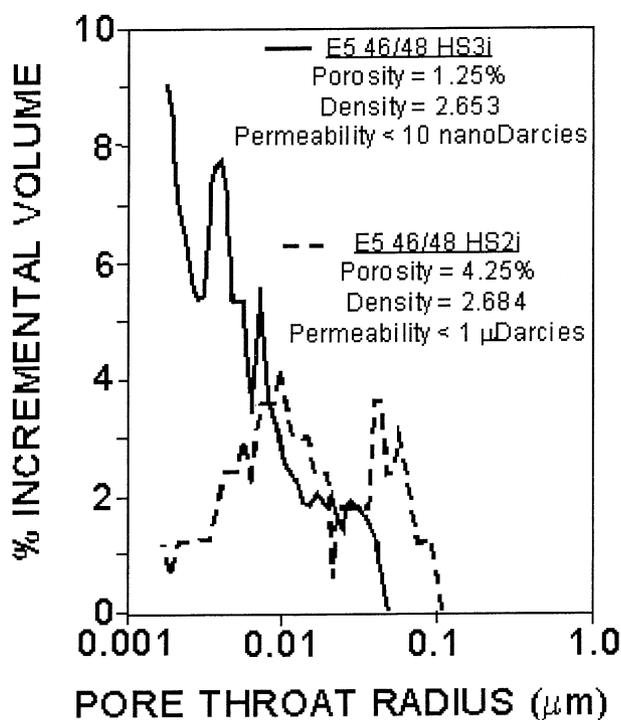
Fig. 3. Hg porosimetry analyses of Carbon Leader sample HS3i and HS2i sample. The pore throat size distributions for HS2i and HS3i were determined by Hg injection capillary pressure analyses (Core Petrophysics, Houston, TX) using the relationship between Hg injection pressure and pore entry radius (Washburn, 1921). Porosity was determined by He and by differences between wet mass versus dry mass, air permeability was measured by air permeameter probe and calculated from the Hg porosimetry data using the approach of Swanson (1981).

was distributed between the oxyhydroxide extraction and more recalcitrant phases, presumably uraninite. The As was equally distributed between the oxyhydroxide extraction and the sulphide extraction.

Microbial enrichments and ^{35}S autoradiography

The enrichment results represent putative presence of the various physiological groups that were targeted by the various enrichment formulas (Table 3), but confirmation by isolation and/or additional analyses for end products was not performed. The service water yielded positive enrichments from room temperature, RT, incubations with both aerobic and anaerobic media in less than two weeks (Table 4). Dilution series analyses indicate that mesophilic, aerobic heterotrophs were present at >10 cells ml^{-1}, and S$^{\circ}$- and thiosulphate-oxidizing bacteria were present at >10^2 cells ml^{-1}. Mesophilic fermenters, nitrate-, Fe(III)-, Mn- and sulphate-reducers were all present at >10^2 cells ml^{-1}. A mesophilic, H$_2$-oxidizer was also detected in the service water. The stope air sample also yielded numerous mesophiles, including H$_2$-, acidophilic S$^{\circ}$- and

Table 2A. Geochemical analyses of pore water from Carbon Leader and quartzite and of service water, dolomite water and fissure water (concentrations in mg l^{-1}).

Rock sample	Method	Porosity	Cl	Br	NO^3	SO^4	Na	Mg	Ca	Fe	Mn	As	U
HS2i	e[a]	0.024	1 451	8.15	0.29	120	490	85	348	0.76	7.44	0.81	0.00
HS2i	c + e[b]	0.01	14 805	77.89	1184	1 792	7765	1010	3602	21.1	185.7	20.42	7.34
HS3p	e	0.022	2 113	9.80	4.13	400	1315	113	1018	81.2	18.9	1.88	56.1
HS3p	c + e	0.01	11 614	88.18	1456	10 877	9552	841	4409	23.42	107.6	38.16	48.35
HS3i	c + e	0.020	9 592	61.42	1176	4 804	8564	392	1456	175	47	438	106
HS2p	c + e	0.01	21 367	78.55	768	767	7210	332	2865	652	58.5	726	358
Water Samples													
U Drill W			300	8.10	37.50	136	N.A.	N.A.	N.A.	N.A.	N.A.	N.A.	N.A.
Final Drill W			300	7.90	37.73	92	N.A.	N.A.	N.A.	N.A.	N.A.	N.A.	N.A.
EDS-1			222	7.85	47.00	40	107	8.4	60	0.30	0.01	0.01	<d.l.
E5-48-SW2			217	10.60	128.00	55	152	10.7	118	0.36	0.02	0.02	0.0610
Dolomite Water[c]			16–53	0.17–0.57	<0.6	39–98	13–17	22–41	37–69	0.22–0.60	0.03–0.06	0.01–0.02	0.001–0.005
E5 Fissure Water[c]			22 600–37 611	106–194	<0.6	46–93	5 710–6390	1.1–1.8	6 789–11 800	28.7–85.3	0.07–0.23	0.04–0.16	0.0001–0.0002

a. e = D.I. water extraction of 5 g of 5 mm chunks.
b. c + e = Crushed to coarse powder and extracted with D.I. water.
c. Summarized in Moser *et al.* (2003).
Anions were measured by I.C.AES (Princeton University) and cations by ICP-MS (Actlabs, Lancaster, Ontario).

Table 2B. Geochemical results of sequential extractions of Carbon Leader and quartzite after D.I. extraction (concentrations in p.p.m.).

Sample	Mn	Fe	S	Al	U	As
MgCl$_2$ extraction[a]						
HS2i	0.43	0.30	<d.l.	<d.l.	1.40	1.25
HS2p	0.36	0.20	<d.l.	<d.l.	1.85	1.90
HS3i	0.38	0.19	9.99	<d.l.	1.93	1.09
HS3p	0.40	0.20	29.95	<d.l.	2.80	3.60
NaClO$_3$ extraction						
HS2i	<d.l.	<d.l.	5 695	5.30	19.80	<d.l.
HS2p	0.20	<d.l.	4 990	16.53	2320	6.20
HS3i	<d.l.	<d.l.	8 283	6.54	987	2.78
HS3p	0.33	<d.l.	10 500	12.50	1803	3.25
NA$_2$S$_2$O$_4$ pH 7 extraction						
HS2i	11.70	1 172	N.A.	42.90	17.20	16.43
HS2p	5.40	4 353	N.A.	115.30	792	114.30
HS3i	8.07	6 721	N.A.	120.60	800	117.20
HS3p	15.30	8 460	N.A.	83.50	2176	96.10
4 N HNO$_3$ extraction						
HS2i	0.79	578	35	524	8.20	<d.l.
HS2p	0.18	76	31	206.6	170.6	0.26
HS3i	1.43	976	105	17.00	467	5.50
HS3p	2.50	3 726	4 590	282.6	855	168.4
Total dissolution of residue						
HS2i	29.40	11	<d.l.	11 199	<d.l.	<d.l.
HS2p	<d.l.	365	<d.l.	5 523	92.00	<d.l.
HS3i	<d.l.	283	<d.l.	5 521	93.90	<d.l.
HS3p-2	1.10	431	<d.l.	6 290	478	<d.l.
TOTAL						
HS2i	42.32	1 761	5 730	11 772	46.60	17.68
HS2p	6.14	4 772	5 021	5 966	3382	122.7
HS3i	9.88	7 940	8 398	5 665	2349	126.6
HS3p	19.63	12 617	15 120	6 669	5315	271.3

All extraction procedures were also applied to a pure pyrite mineral standard.

thiosulphate-oxidizers, aerobic heterotrophs, fermenters and Fe(III)- and sulphate-reducers (Table 4).

The 60°C enrichments of the service water yielded far fewer indications of growth. A rod-shaped, thiosulphate-oxidizer, 1–2 μm long, was present at >1 cells ml^{-1}. The aerobic and anaerobic *Sulfolobus* media yielded growth at >10^2 cells ml^{-1} and >10 cells ml^{-1} respectively. No thermophilic, aerobic heterotrophs, nitrate or Mn reducers were detected (<1 cell ml^{-1}), but thermophilic Fe(III)- and sulphate-reducing media did yield filamentous, Fe(III)-reducers and rod-shaped sulphate-reducers, respectively, at >1 cell ml^{-1} and <10^2 cells ml^{-1} (Table 4). The only thermophile enriched in the stope air sample was a large, 1×5 μm, rod-shaped, Fe(III)-reducer (Table 4).

For the external parings and internal chunks of Carbon Leader, mesophilic enrichments consistently yielded more positives over a shorter incubation period than did the 60°C enrichments. Even the tracer free, internal chunk of the Carbon Leader block sample (HS3i in Table 4) yielded positive results (10^2 > >1 cell g^{-1}) for mesophilic thiosulphate-, S°- and H$_2$-oxidizers, for aerobic heterotrophs, for fermenters and for nitrate-, MnO$_2$-, Fe(III)- and sulphate-reducers and methanogens. This sample yielded positive 60°C results for H$_2$-oxidizers, fermenters, all of the Fe(III) reducing media, MnO$_2$ reducers,

sulphate reducers and methanogens (10^2 > >1 cell g^{-1}; Table 4). The HFO media yielded 1–2 μm long, rod-shaped cells and the MnO$_2$ reducing media yielded 1–3 μm long, rod-shaped cells. Clusters of 5 μm long, rod-shaped, thermophilic sulphate-reducers and fermenters were also present in enrichments of the internal chunks of the Carbon Leader cores (E5-46–48-RC-0.7i and 0.8i in Table 4).

Autoradiographic analyses using ^{35}SO$_4$ failed to detect 60°C sulphate reduction activity in the internal chunk of the Carbon Leader (HS3i), but did detect localized activity in a carbon-rich pore for an external chunk (HS4 in Fig. 4B).

The internal chunk of the quartzite block sample yielded mesophilic fermenters, Fe-citrate, MnO$_2$ and sulphate reducers, and 60°C fermenters, Fe-citrate and sulphate reducers (HS2i in Table 4). Low levels of sulphate reduction were also detected by ^{35}S autoradiography at 60°C in the quartzite (Fig. 4A).

PLFA analyses

The service water and drill water PLFA concentrations ranged from 1.61 to 79.49 pmole ml^{-1}. The maximum value was found in the condensate collected from the surface

return air fan, E2-0-FD1. The next highest biomass value was 50.44 pmole ml^{-1} for EDS-1, which was service water collected from the plumbing that carried it to the stope. The second and final drilling water samples yielded lower concentrations of 20.00 and 11.00 pmole ml^{-1} respectively. These are higher than the initial drilling water (First DW, 2.23 pmole ml^{-1}) spiked with Rhodamine WT and fluorescent microspheres. Service water emanating from a hose in the stope and used to rinse HS2 and HS3 yielded the lowest PLFA concentration, 1.61 pmole ml^{-1}.

The most abundant PLFA's in the service water and fan drift condensate were the normal saturates (30–59%) and the monoenoics (24–55%), indicative of Gram-negative bacteria (Fig. 5). Mid-branched saturates were also common in all samples but represented a relatively minor component. Terminally branched saturates, indicative of Gram-positive and some anaerobic bacteria, were also a relatively minor component in the stope service water, but comprised 5–8% of the PLFA in the fan drift condensate and the water in the circulation loop. Branched monoenoics were negligible in all service water samples. Polyenoic PLFA's, indicative of eukaryotes, were significant in the fan drift condensate and all service water samples with the exception of EDS-1. The proportion of polyenoic PLFA was highest in the drill water samples collected after intersection with the fluid-filled fracture (U Drill W and Final Drill W), attaining up to 13% (Fig. 5). Of the other PLFA's detected, the most significant were the oxiranes (formed by chlorine disinfection of the service water), which comprised up to 27% of EDS-1 and were detected in the drilling water, but were absent from the stope water and fan condensate samples.

Total PLFA was highest for rock samples from the access tunnel walls, yielding 81 pmoles/g for a quartzite (Quartz-Fe in Fig. 5) and 18 pmoles/g for Carbon Leader samples. Carbon Leader that was chiseled from a 2-month-old stope face (E5-46/48-CLE1 in Figs 1 and 5) yielded a concentration of 0.7 pmoles/g. The PLFA concentrations for the Carbon Leader block sample correlated with proximity to the service water-rinsed surface, with HS3p yielding 13 pmoles/g, HS4 yielding 1 pmole g^{-1} and HS3i yielding the lowest PLFA value of the data set (0.3 pmole g^{-1}). The internal chunk of the quartzite block sample yielded 5 pmole g^{-1}. The parings to the core samples (E5-46/48-RC0.7p and 0.8p in Fig. 5) yielded PLFA concentrations of 4 and 6 pmole g^{-1}, whereas, the internal core chunk yielded only 0.4 pmole g^{-1}.

The most abundant PLFA's for the rock samples were the normal saturates (24–89%), the monoenoics (8–45%) and the polyenoics (2–23%). The mid-branched and terminally branched saturates and branched monoenoics were minor constituents (<3%) in some of the rock samples (Fig. 5). The PLFA profiles for the rock parings were very similar to the internal chunks, with one exception.

HS3p contained 10% oxiranes, but oxiranes were absent from HS4 and HS3i (Fig. 5).

All service and drill water samples and one quartzite sample from the access tunnel wall clustered together under a linkage distance of 40 in Fig. 6. Carbon Leader block samples, HS3p, HS3i, and HS4, showed a distant relationship (linkage distance of 70 in Fig. 6) to the service and drill water samples. This relatedness is a result of the higher relative abundances of monoenoics and polyenoics found in these samples compared to the Carbon Leader core samples and the quartzite block sample. These latter samples were not related (linkage distance 136 in Fig. 6) to the service and drill waters, because their PLFA profiles contained higher relative abundances of normal saturates.

DNA analyses

16S rDNA was sequenced for clone libraries from two service water samples, one air sample, the internal chunk of the Carbon Leader block and stope face samples (HS3i and 3–3CLi in Table 5). The sequences were subdivided into 45 bacterial clone types and seven archaeal clone types (Table 5; Takai *et al.*, 2001a). Clone types 3 through 5 and 32 belonged to the α-*Proteobacteria* division, 6 through 18 belonged to the β-*Proteobacteria* division, 20 through 30 belonged to the γ-*Proteobacteria* division and the remaining clone types to other divisions within *Bacteria* or *Archaea* domains (Table 5).

The clone types that were strictly associated with the service water included:

1. Type 7a which appears to be an *Alcaligenes* species in the *Bordetella* Group.
2. Type 10b, which was most similar to *Hydrogenophaga* sequences.
3. Type 13a, which fell within but was not closely related to any member within the *Acidovorax* Group.
4. Type 16c, which was deeply branching within the β-*Proteobacteria* division and could not be assigned to any group with certainty (Fig. 7A).
5. Type 17, which was deeply branching within the *Methylophilus* Group.
6. Type 24, which was a deeply branching species of *Acinetobacter* Group.
7. Type 30a, which appeared to be a member of the genus *Pseudomonas* (Fig. 7A).
8. Type 28, which branched deeply within the *Thiocapsa reopersicina* Group.
9. Type 30b, which was deeply branching within the *Proteobacteria* division and cannot be assigned to any group with certainty (Fig. 7A).
10. Type 30c, which was related to *Nevskia ramosa* (Fig. 7A).
11. Type 36d, which appeared to represent a new taxon within the δ-*Proteobacteria* (Fig. 7B).

Table 3. Composition for microbial enrichment media.

Reference	T. dentrif (Atlas, 1993)	H_2+O_2 (Atlas, 1993)	So oxi. (Atlas, 1993)	So red. (Myers and Nealson, 1988; Moser and Nealson, 1996)	Sulf. Aero (Robb, 1995)	Sulf. Anaero (Robb, 1995)	Aero TYG	Anaero TYG	Anaero TYEG	NRB (Tiedje, 1982)	Basal FeHFO — HFO	Basal FeHFO — Fe NTA	Basal FeHFO — NTA	Basal FeHFO — PIPES (Kieft et al., 1999)	Fe citrate	Mn red. (Postgate, 1984)	SRB	SRB/Meth.	H_2/CO_2
Methanol																			20 mM
Na Acetate				10 mM							10 mM	10 mM	0.12 mM	10 mM	10 mM	10 mM	10 mM	10 mM	
Na Lactate				10 mM							10 mM	10 mM	0.12 mM	10 mM	10 mM	10 mM	10 mM	10 mM	
Na Pyruvate				10 mM							10 mM	10 mM	0.12 mM	10 mM	10 mM	10 mM	10 mM		
Yeast Extract					2	2	3	3	0.1		1			1	1	1		0.005	0.01
Tryptone					2	2	5	5	0.05										
Peptone									0.05										
Glucose							1	1	0.1										
Sucrose					2	2	2												
Nutrient Broth																			
$Na_2S_2O_3 \cdot 5H_2O$	5																		
KNO_3	0.5							1		3									
HFO										0.5	2.3			2.3					
Fe(III) citrate															12.3				
Fe(III) NTA						1.6						10 mM	0.12 mM						
MnO_2													0.12 mM			0.87			
Na_2SO_4																	1		
$CaSO_4$																	0.44	2.85	
$MgSO_4 \cdot 7H_2O$	0.2		0.3		1.6				0.06				0.1				0.5		
$FeSO_4 \cdot 7H_2O$	0.005																		
S°			10	1.4													1		
NH_4Cl	0.25				1.6						1.5	1.5	1.5	1.5	1.5	1.5	1		
$(NH_4)_2SO_4$			0.3																
Vitamins									10 ml		10 ml	10 ml	10 ml	10 ml	10 ml	10 ml	10 ml*	10 ml	10 ml
Minerals									10 ml		10 ml	10 ml	10 ml	10 ml	10 ml	10 ml	10 ml	10 ml	10 ml
Trace Elements	0.25 ml																		
Trace Metals		1 ml																	
$NaHCO_3$	0.5	0.5									2.5	2.5	0.5		2.5	2.5		0.85	0.85
Na_2CO_3		9									0.6	0.6		0.6	0.6	0.6			
$NaH_2PO_4 \cdot 12H_2O$					0.28	0.28							0.42				0.5		
Na_2HPO_4									0.142				1.8					0.142	0.142
Na_2PO_4																			
K_2HPO_4	0.5	1.5	3						0.174									0.174	0.174
PIPES									0.1					10 mM				0.1	0.1
MOPS																			

pH	6	7	4.8	7.5	3–3.5	7	7	7	7.8	5.5	7.8	6.5	6.5	7	7.8	7.8	7–7.5	7.8	7
NaCl									0.07									0.9	0.9
KCl															0.1			0.2	0.2
$MgCl_2 \cdot 6H_2O$																		0.1	0.1
$CaCl_2 \cdot 2H_2O$																			

Amounts given in table are in grams per litre unless stated otherwise.

Trace metal solution was comprised of 50 g l⁻¹ disodium EDTA, 22 g l⁻¹ $ZnSO_4$, 5.54 g l⁻¹ $CaCl_2$, 5.06 g l⁻¹ $MnCl_2$, 4.99 g l⁻¹ $FeSO_4 \cdot 7H_2O$, 1.61 g l⁻¹ $CoCl_2$, 1.57 g l⁻¹ $CuSO_4$ and 1.1 g l⁻¹ $(NH_4)_2MoO_4$ and the pH was adjusted to 6.0 with KOH.

Trace element solution was composed of 0.03 g l⁻¹ $MnCl_2$, 0.02 g l⁻¹ $NiCl_2 \cdot 6H_2O$, 0.1 g l⁻¹ $ZnSO_4 \cdot 7H_2O$, 0.02 g l⁻¹ $CuCl_2 \cdot 2H_2O$, 0.02 g l⁻¹ $CoCl_2 \cdot 6H_2O$, 0.3 g l⁻¹ H_3BO_3 and 0.03 g l⁻¹ $NaMoO_4$.

Mineral and vitamin solutions are from Wolin et al. (1963).

PIPES is piperazine-N,N'-bis2-ethanesulphonic acid.

MOPS is 3-[N-morpholino]propanesulfonic acid.

NRB had 1 ml l⁻¹ of diphenylamine reagent as an indicator of nitrate removal.

SRB had an addition 0.1 g l⁻¹ ascorbic acid and 0.1 g l⁻¹ of Thioglycollic acid.

To inhibit methanogens, 1.05 g l⁻¹ 2-bromoethanesulphonic acid sodium salt (BESA) as added to the Fe(III)-citrate reducing media.

1 ml of Resazurin (0.1% stock solution) was used as a redox detector in the anaerobic media.

0.5 g l⁻¹ Cysteine HCl was added as a reductant to the fermentative and sulphate and CO_2 reducing media to remove any trace O_2.

A

B

Fig. 4. Autoradiographic scan of Ag foil and photo of (A) HS2i rock face and (B) HS4 rock face. Rock samples were stored at 4°C under N_2 before analysis. They were fractured with a sterile chisel in the anaerobic glove bag. One of the fresh faces was then coated with a sterile solution of 2.5 µCi (HS-2i and HS-4) or 7.5 µCi (HS-3i) $Na^{35}SO_4$ in anoxic (N_2 purged) D.I. water. The rock fragments were then covered with a piece of Ag foil treated as previously described (Krumholz *et al.*, 1997) were reassembled along the fracture and then covered with Al foil and taped together. These were incubated for 25 days under N_2 in a sealed box at 56°C. The Ag foil was subsequently removed and washed in D.I. water to remove sulphate. The radioactive sulphide trapped on the Ag foil was imaged by electronic autoradiography using an Instantimager (Packard Instrument, Meriden, CT).

The clone types that were strictly associated with the stope air included:

1. Type 32, which fell within the *Rhodopila* Group, but was too deeply branching to be placed within any genus of that group.
2. Types 8 and 13d, which fell within but were not closely related to any known species of the *Nitrosomonas* Group.
3. Type 15, which fell within the *Leptothrix* subgroup of the *Acidovorax* Group.
4. Types 27a, 27b, and 27c, which fell within the *Xanthomonas* Group, but were distant from known representatives (Fig. 7A).
5. Types 36a, 36b and 33, which fell within the Chlorobi and Relatives (Fig. 7B). Types 36a and 36b were

Table 4. Microbial enrichments.

Sample	T°C Sal.	g or ml	T. dentrif.*	H₂+O₂ **oxi.	S° red.	S° Aero	Sulf. Anaero	Sulf. TYG	Aero TYG	Anaero TYEG	Anaero ***	NRB HFO	Fe NTA HFO	Fe NTA	Basal HFO	Pipes + citrate	Fe red.	Mn SRB	Meth.	SRB/ H₂/CO₂
E5-46/48-CL-E1	60	1.23	–	–	–	NA	+	–	–	–	+	–	+ –	NA	+	+	+	+	–	NA
E5-46/48-CL-E1	60	0.06	NA	NA	–	NA	+	+	NA	–	+ –	–	NA	NA	–	–	–	–	–	–
E5-48-CL	RT	0.1	NA	NA	NA	NA	NA	NA	+	+	NA	+	+ –	NA	+	+	NA	+	+	NA
E5-48-CL	60	0.1	NA	NA	NA	NA	NA	NA	–	+	NA	+	+ –	NA	–	–	NA	–	+	NA
E5-48-3-3	RT	0.1	NA	NA	NA	NA	NA	NA	+	+	NA	+	+ –	NA	–	–	NA	–	+	NA
E5-48-3-3	60	0.1	NA	NA	NA	NA	NA	NA	–	–	NA	–	+ –	NA	–	–	NA	–	–	NA
3–3 CLi	60	0.1	–	–	NA	NA	NA	NA	NA	NA	NA	NA	+ –	+	+ –	+ –	–	+	–	NA
4–2 CL	60	1	–	–	–	NA	+	+	NA	+	+ –	–	+	+	–	+	+	+	+	+ –
HS4i	RT	0.6	+	NA	+	NA	–	+	–	+ –	+	–	+	NA	–	–	+	–	+	+ –
HS4i	60	0.6	–	–	–	NA	+	–	+	NA	+	–	+ –	NA	–	–	+ –	+	+	+ –
HS3i	RT	1.02	+	+	+	–	+	–	+	+	+	+	+ –	+	–	+ –	+ –	+	–	+ –
HS3i	60	1.02	–	+ –	–	NA	–	–	–	+	+	–	+ –	+	–	+	+ –	+	–	+ –
HS2i	RT	1.71	–	NA	–	NA	–	–	+	NA	+	–	–	NA	–	–	+ –	+	–	+
HS2i	60	1.71	–	–	–	NA	–	–	–	–	+	–	+ –	NA	–	–	+ –	–	–	+
E5-46–48-RC-0.7i	60	1	+	NA	NA	NA	+	–	–	+ –	–	–	+ –	+ –	–	+ –	–	–	+	–
E5-46–48-RC-0.7i	60 w/NaCl	1	–	NA	NA	NA	+	–	NA	+ –	–	NA	NA	+ –	–	NA	–	–	+	NA
E5-46–48-RC-0.8i	60	1	–	NA	–	NA	+	–	–	+ –	+	–	+ –	+	–	+ –	+	+	–	NA
E5-46–48-RC-0.8i	60 w/NaCl	1	–	NA	–	NA	+	–	NA	+ –	+	NA	+ –	NA	NA	NA	+ –	–	–	NA
E5-46-SW2	RT	1	+	+	+	NA	+	+	+	+	+	+	?	+	+	+	+	+	–	+
E5-46-SW2	RT	0.1	+	NA	–	NA	+	+	+	+	+	+	?	+	+	+	+	+	+	+
E5-46-SW2	RT	0.01	+	NA	–	NA	+	+ Clost.	–	+	–	+	?	+	+	+	+	+	+ –	+ –
E5-46-SW2	60	1	–	–	–	NA	+	–	–	–	–	–	–	+	–	–	+	–	+	+
E5-46-SW2	60	0.1	+	NA	+	NA	+	+	+	+	+	–	–	+	+	+	+	–	–	+ –
E5-46-AIR	RT	NA	+	+	+	–	+	+	+	+	+	–	–	NA	NA	+	–	–	+	NA
E5-46-AIR	60	NA	–	NA	–	NA	–	–	–	+	–	–	–	NA	NA	–	+ –	–	–	NA
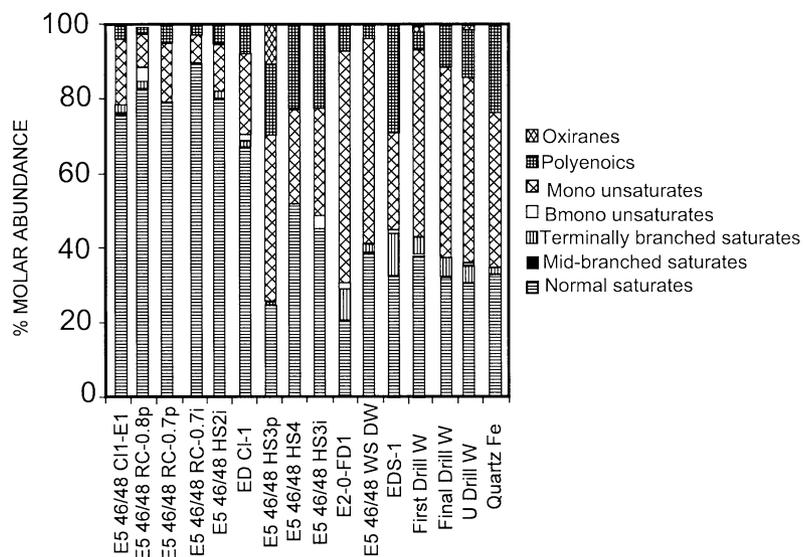
Fig. 5. Molar proportions of PLFA groups for service water, Carbon Leader and quartzite samples. Service water, air, Carbon Leader and quartzite PLFA biomass concentrations in pmole ml^{-1} were 1.61 for E5-46/48 WS DW, 2.23 for First DW, 20.05 for U-Drill W, 11.53 for F-Drill W, 50.44 for EDS1, 79.49 for E2-0-FD1, 18.57 for EDCL-1, 12.65 for E5 46/48 HS3p, 1.41 for HS4, 0.33 for HS3i, 0.65 for E5 46/48CL1-E1, 5.77 for E5 46/48 RC0.7p, 0.44 for E5 46/48 0.7i, 4.97 for E5 46/48 HS2i and 81.28 for Quartz 5FE,

deeply branching within that group; whereas type 33 may be a *Thermus* or *Meiothermus* strain.

6. Type 35, which fell within the *Bacteroidetes* Group, but appeared unrelated to known members (Fig. 7B).

7. Type 36c, which branched deeply within the Eubacteria and could not be placed with certainty into any of the major phyla (Fig. 7B).

The clone types that were associated with both the service water and stope air included:

1. Types 3 and 4 which belonged to the *Sphingomonas* group of the α-*Proteobacteria* division (Table 5; Fig. 7A).

2. Types 5b, 5c, and 5d were all rather deeply branching within the *Rhodobacter-Rhodovulum-Hyphomonas-Rickettsia* Group (Fig. 7A).

3. Types 6, 7b, 8 and 13d, which belonged to the *Azoarcus* Group, *Bordetella* Group and *Nitrosomonas* Group of the β-*Proteobacteria*, respectively (Fig. 7A).

The clone types that were strictly associated with Carbon Leader internal chunks included:

1. Type 9, which was the dominant clone type in both samples and was most similar to the *Acidovorax* species LW1 (Katsivela *et al.*, 1999).

2. Type 21, which was the second most abundant type in both samples and was a nearly exact match to *Pseudomonas stutzeri* and *Pseudomonas balaerica* (Fig. 7A).

3. Types 20, which were the third most abundant type in
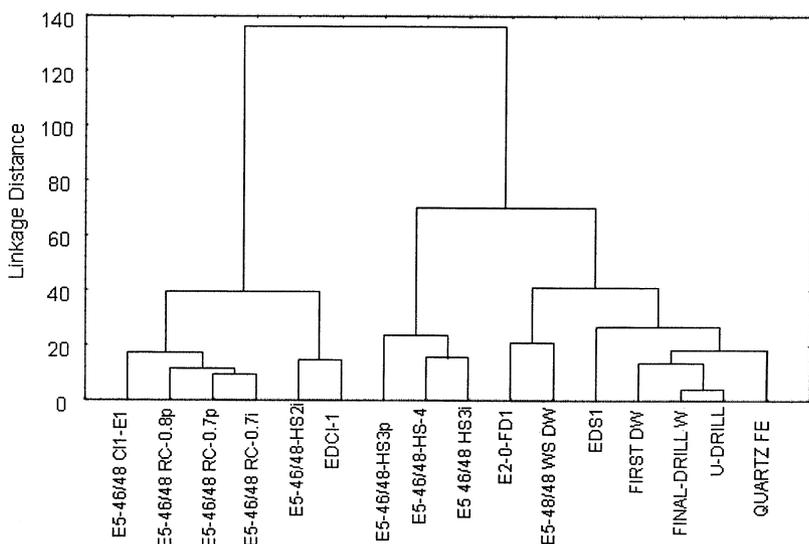
Fig. 6. Hierarchal cluster analyses of PLFA data for Carbon Leader, quartzite and service water samples.

Table 5. 16S rDNA clone library.

Clone type	RF (bp)	General phylogenetic	Position of clone(s)	Service EDS 1.	Water E5–46 / SW2	Air E5–46	Carbon E5–46 / HS3i4	Leader 3–3 / CLi
3a	81	α-*Proteobacteria*	*Sphingomonas Gp.*		2[a]			
3b	81	"	*Sphingomonas Gp.*		1			
4	71	"	*Sphingomonas Gp.*		1			
5a	39	"	*Rhodobacter*					1
5c	39	"	*Rhodobacter-Rhodovulum-Hyphomonas-Rickettsia*		1			
5d	39	"	*Rhodobacter-Rhodovulum-Hyphomonas-Rickettsia*			1		
5b	39	"	*Rhodobacter-Rhodovulum-Hyphomonas-Rickettsia*			1		
32	62	"	*Rhodopila Gp.*			2		
6	77	β-*Proteobacteria*	*Azoarcus Gp.*		1			
7a	67	"	*Bordetella Gp. Alcaligenes Sp.*	1[b]	1			
7b	200	"	*Bordetella Gp. Bordetella Sp.*				1	
8	207	"	*Nitrosomonas Gp.*			1		
9	205	"	*Acidovorax Gp. Acidovorax Sp.*LW1				38	1
10a	69	"	*Acidovorax Gp. Hydrogenophaga Sp.*					1
10b	69	"	*Acidovorax Gp. Hydrogenophaga Sp.*		2			
13a	149	"	*Acidovorax Gp.*		1	5		
13b	199	"	*Acidovorax Gp, Leptothrix SubGp.*					1
13c	52	"	Uncertain placement			1		
13d	207	"	*Nitrosomonas Gp.*			1		
14	219	"	Environ. clone ACK-C30 U85120	3[b]	4		1	
15	198	"	*Acidovorax Gp, Leptothrix SubGp.*			4		
16a	200	"	Uncertain Placement				1	
16b	221	"	Uncertain Placement					1
16c	225	"	Uncertain Placement		2			
17	202	"	*Methylophilus Gp.*		1			
18	219	"	*Methylophilus Gp. Methylophilus methylotrophus Sp.*				2	
20	206	γ-*Proteobacteria*	*Pseudomonas* and Relatives Gp. *Acinetobacter junii*				17	1
21	39	"	*Pseudomonas* and Relatives Gp. *Ps. stutzeri Sp.*				17	2
23	200	"	*Pseudomonas* and Relatives Gp. Acinetobacter				1	
24	394	"	*Pseudomonas* and Relatives Gp. Acinetobacter?		1			
30a	39	"	*Pseudomonas* and Relatives Gp. *Pseudomonas*	2[b]	1			
26	39	"	*Enterics* and Relatives Gp. *Serratia*					1
27a	38	"	Xanthomonas Gp.			1		
27b	38	"	Xanthomonas Gp.			2		
27c	38	"	Xanthomonas Gp.			1		
28	47	"	*Thiocapsa reopersicina* Group		1			
29	69	"	Uncertain Placement				14	
30b	39	"	Uncertain Placement		1			
30c	194	"	*Nevskia ramosa*		1			
36d	257	δ-*Proteobacteria*	Uncertain Placement		1			
33	197	*Chlorobi*	*Thermus* or *Meiothermus G.*			16		
36a	232	*Chlorobi*	Uncertain Placement			1		
36b	232	*Chlorobi*	Uncertain Placement			1		
35	39	*Bacteroidetes*	Uncertain Placement			9		
36c	206	*Eubacteria*	Uncertain Placement			1		
4–7-J2[c]	N.A.	*Euryarchaeota*	*Methanobacterium hungateii*	24				
L-N[c]	N.A.	"	*Methanoseata concilli*	9				
MO6[c]	N.A.	"	*Methanosarcina frisius*	3				
P[c]	N.A.	*Crenarchaeota*	*>97%* Soil group	2				
8[c]	N.A.	"	Marine Group I pIVWA5	6		28		
9[c]	N.A.	"	Marine Group I APA3-0	1		1		
37	N.A.	"	DHVE3			12		

a. No. of clones per sample.
b. Correlation is based upon T-RFLP.
c. Clone type designations from Takai *et al.* (2001a).

both samples, and 23, both of which were species of *Acinetobacter* in the *Pseudomonas* and Relatives group (Fig. 7A).

4. Type 29, which was the fourth major clone type in HS3i and was very deeply branching within the γ-*Proteobacteria* (Fig. 7A).

5. Type 5a, which was from 3-3CLi and related to a *Rhodobacter* species.

6. Type 7b, which was from HS3i and may have been a *Bordetella* species.

7. Type 10a, which was from 3-3CLi and was most similar to *Hydrogenophaga* sequences.

A
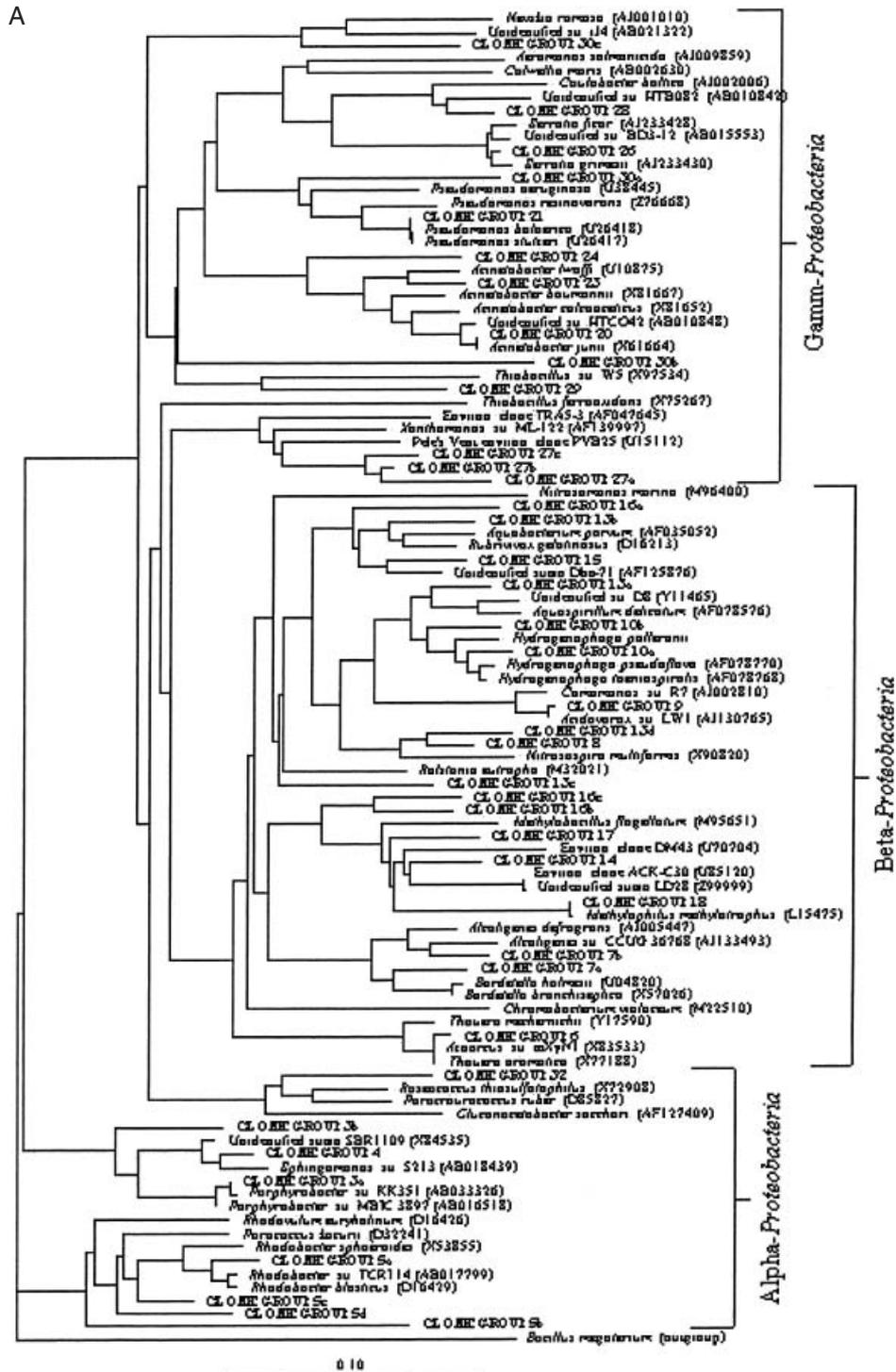
Fig. 7. A. Distance matrix tree for Proteobacteria sequences.

8. Type 13b, which fell within the *Leptothrix* subgroup of the *Acidovorax* Group.
9. Types 16a and 16b, which were deeply branching within the β-*Proteobacteria* division and cannot be assigned to any group with certainty (Fig. 7A).

10. Type 18, which was nearly identical to *M. methylotrophus*.
11. Type 26, which was from 3-3CLi, fell within the Enterics and Relatives (RDP), and appeared to be a species of *Serratia*.
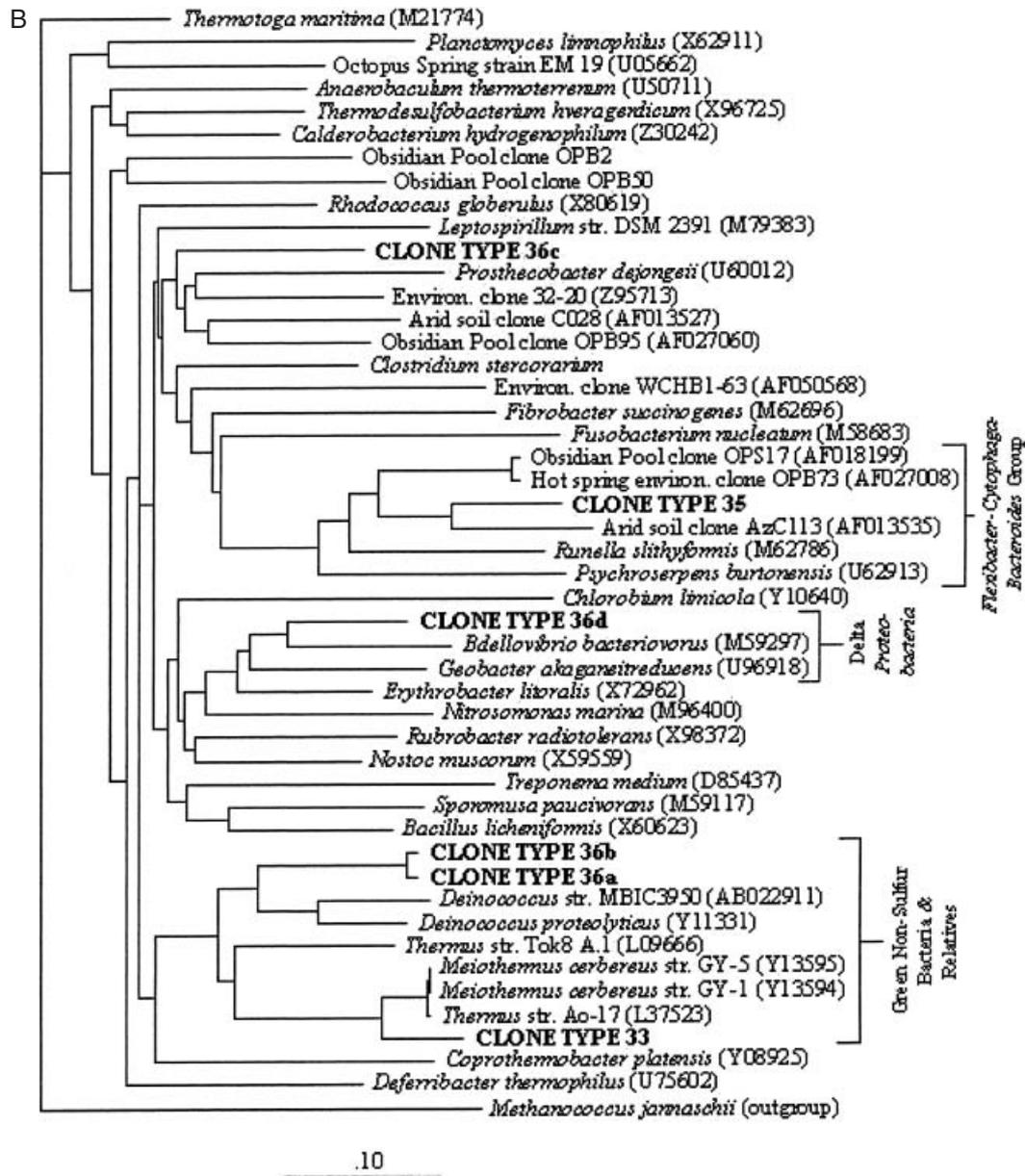
Fig. 7. B. Distance matrix for miscellaneous bacterial clones. phylip (Felsenstein, 1993) was used for distance matrix analyses. Distances were calculated by the method of Jukes and Cantor (1969) after which phylogenies were estimated with the algorithm of Fitch and Margoliash (1967). Parsimony analyses were carried out with the paup program (paup 4.0, beta version 8; Sinauer Associates, Sunderland, MA), using the standard program defaults for heuristic searches. Maximum likelihood analyses were performed with the DNAML option in phylip using the standard program defaults. The branch nodes in the phylogenetic trees generated by distance matrix and parsimony analyses were further evaluated by bootstrapping data at the >50% confidence limits, with 100 replications (Felsenstein, 1985).

The only clone type that was associated with both the Carbon Leader and service water samples was type 14, which was most closely related to an environmental strain and distantly related to the *Methylophilus* Group (Fig. 7A).

T-RFLP electropherograms of the service water samples yielded a total of 197 ribotypes (Fig. 8) of which 24 were correlated to ribotypes from the clone library. Of these 24 peaks, seven represented more than one clone type from the clone library. The air sample T-RFLP elec-

tropherogram yielded 21 peaks (Fig. 8). The 3–3CLi T-RFLP electropherogram contained 81 peaks and that of HS3i contained 70 peaks (Fig. 8).

Discussion

Mining contaminants

The service water contained elevated concentrations of Br, NO_3 and SO_4 and its Br/CL was much greater than that

T-RF Length (bp)
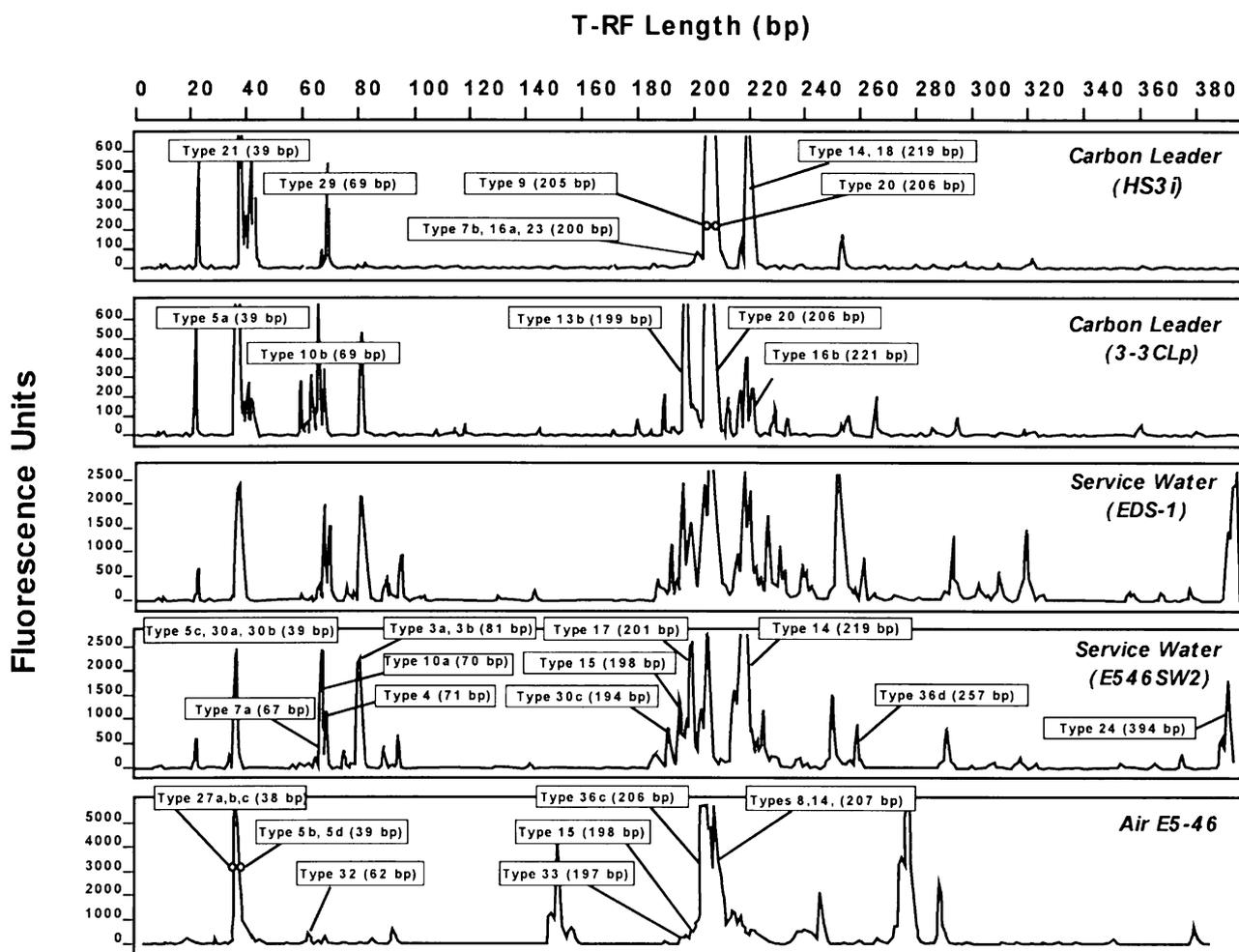
Fig. 8. T-RFLP of service water and Carbon Leader samples. Peak selection was based on using 12 Genescan units as a baseline.

of either highly saline fissure water or low salinity dolomite water at this mine (Table 2A). The two service water samples yielded very similar bacterial clone libraries with great diversity, dominated by groups within the *Proteobacteria*, including *Sphingomonas*, *Acidovorax* Gp. *Hydrogenophaga* Sp. and *Pseudomonas*. In contrast, the stope air yielded some clone types similar to those seen in the service water library, such as *Acidovorax* Gp., but the dominant types, which included the *Nitrosomonas* Gp., *Leptothrix* SubGp., *Xanthomonas* Gp., known *Thermus* species and members of the *Bacteroidetes* Gp., were not found in either service water clone library. T-RFLP analyses of the service water revealed more ribotypes than were represented in the clone library, and some T-RF's were the same lengths as those expected from the Carbon Leader and air clone libraries. Whether the latter means that ribotypes from the Carbon Leader and air are present in the service water or that other species distinct from any found in the clone libraries exist in the service water cannot be determined.

The community composition inferred from the clone library is consistent with the dominant PLFA components, which are indicative of Gram-negative bacteria. Tuberculostearic acid (10me18:0), which is a marker for Actinomycetes and *Mycobacterium*, was only detected in EDS-1 and E2-0-FD1, but not in the stope service water, suggesting this bacterial component is introduced into the mine, but does not prosper in the stopes. This is consistent with its absence from the clone libraries.

The difference between the service water and stope air samples was also detected in the archaeal clone libraries and T-RFLP electropherograms. In EDS-1 methanogen sequences (e.g. *Methanobacterium hungateii*) dominated the archaeal community; whereas, in the air sample, Marine Group I *Crenarchaeota* dominated the archaeal community.

The best estimates of the microbial biomass are derived from the PLFA concentrations. For the purpose of this discussion, they are converted into cells ml^{-1} or cells g^{-1} by multiplying by 25 000 cells pmole^{-1} (White and

Ringelberg, 1998). The biomass concentration in the service water samples ranged from 4×10^4 to 1.0×10^6 cells ml^{-1}. The archaeal 16S rDNA comprised only 0.1% of the total DNA of the service water (Takai *et al.*, 2001a) or $\sim 0.04 - 1 \times 10^3$ archaeal cells ml^{-1}. The fan drift condensate and the service water in the circulation system yielded higher biomass concentrations than the service water used in the stopes. The stope water biomass concentration is 100× less than that typical of drilling mud used in deep drilling (Colwell *et al.*, 1997; Onstott *et al.*, 1998b). This trend also holds true for PLFA biomarkers for anaerobes and the polyenoic marker for fungus. This suggests that contaminating microbial contaminants entering the service water on the return path and at the surface are being significantly reduced in the circulation system by the chlorine and bromine additions before arriving at the stope.

Almost one-third of the clone types in the service water and air could not be correlated confidently with any groups within the bacterial phyla, which hampers the inference of their environmental role. The sequences most similar to those in the RDP database included *Porphyrobacter* species and members of the *Rhodobacter* and *Azoarcus* groups suggesting the service water is populated by aerobic heterotrophs. This result is consistent with RT enrichments, although MPN estimated concentrations of 10–100 cells ml^{-1} are only a minor fraction of the total viable population estimated from the PLFA. The presence the *Nitrosomonas* group in the air sample may be consistent with the contamination of the air with explosive residues of NH_3 that in conjunction with O_2 could be used by nitrifying bacteria for growth. The concentrations of terminally branched saturate and monoenoics PLFA's in the service water imply that 10^4– 10^5 cells ml^{-1} of anaerobic sulphate- and metal reducing-bacteria may be present. Anaerobic enrichments confirm the presence of mesophilic sulphate-, Fe(III)- and MnO_2-reducing organisms at $>10^2$ cells ml^{-1} and of thermophilic Fe(III)- and sulphate-reducing microorganisms and fermenters at concentrations of <10 cells ml^{-1} (Table 4). The clone types whose correlation within the bacterial phyla or groups was uncertain may represent these anaerobic respirers. The PLFA biomarker for *Desulfobacter* (10me16:0) concentration was highest in the fan drift water, lower in EDS-1, equivalent to 10^4 cells ml^{-1}, and absent from the stope water. The 10me16:0 only comprised 0.7% of the total PLFA of EDS-1, however, so the absence of any δ-*Proteobacteria* sequences in its clone library is not surprising.

Rock and fracture water geochemistry and microbial composition

The pore water Br/CL of the internal chunks of the Carbon Leader and quartzite is comparable to that of saline fissure water encountered in Witwatersrand strata (Moser *et al.*, 2003) and distinct from either service water or dolomite water (Table 2A). The pore water sulphate was greater than the service water sulphate and it was even higher in the crushed rock leachate suggesting that some of the sulphate originates from the fluid inclusions. The sulphate concentration also correlated with the U concentration in the rock. Sulphate ranging from 1000 to 17 000 p.p.m. have been reported for fluid inclusions in hydrothermal quartz samples from the Witwatersrand sequence and attributed to a non-specific, *in situ* oxidation process. Pore water nitrate was much lower than that of the service water. Nitrate concentrations in the crushed rock leachate were higher than the pore water, suggesting that some nitrate may also be present in the fluid inclusions. Frimmel *et al.* (1999) reported 495–4352 p.p.m. of nitrate for fluid inclusions in hydrothermal quartz veins from the Witwatersrand Supergroup. The pore water Fe concentrations were higher than that of the service water, dolomite water, but similar to that of the Ventersdorp brines. Intriguingly, most of the solid-phase Fe was not associated with the sulphide phases but was present as oxides, the concentrations of which correlated with U. The pore water chemistry, however, suggests that these Fe oxides are not the result of oxidation by mine service water or air.

The major clone types unique to the Carbon Leader libraries included *Acidovorax*, *Acinetobacter junii* and *Ps. stutzeri* species and a very deeply branching γ-*Proteobacteria*. The fact that the T-RFLP electropherograms of HS3i and 3–3CLi resembled those of the service water suggested that the bacteria in the Carbon Leader samples had a common origin. Only 14 of the 81 3–3CLi T-RFLP peaks and 16 of the 70 HS3i T-RFLP peaks did not match a service water T-RFLP peak (Fig. 8). The dominant peaks of the Carbon Leader T-RFLP, 197, 205, 207 bp and 219 bp, coincided with dominant peaks in the service water T-RFLP, but only the 219 bp peak corresponded to a service water clone (type 14) and none coincided with air clones. Consequently, inference from the T-RFLP profiles of similarity in microbial communities between the Carbon Leader and service water relies upon the ribotypes at 197, 205 and 207 bp in the Carbon Leader T-RFLP actually representing uncloned service water microorganisms. Of the 16 T-RFLP peaks uniquely associated with the Carbon Leader samples, 6 were common to both samples and comprised only 2.7% of the total peak area, which probably explains why none of the sequences from the Carbon Leader clone library match any of these T-RFLP peaks. No *Archaea* 16S rDNA were detected by PCR of the DNA extracted from either HS3i or 3–3CLi.

The range in total PLFA for the rock samples is very similar to that found for the Mponeng rock samples (Onstott *et al.*, 1997). The Carbon Leader samples from Drie-

fontein are composed primarily of normal saturates and monoenoics, similar to the 38–64% normal saturates and 37–40% monoenoics for Mponeng Carbon Leader samples and consistent with a Gram-negative bacterial population. One of the Mponeng Carbon Leader samples contained 21% polyenoics very similar to that observed in our Carbon Leader block samples (HS3 and 4 in Fig. 5). Because that Carbon Leader sample yielded a 16S rDNA sequence that was somewhat similar to cyanobacteria, the polyenoics were interpreted as representing a cyanobacteria membrane signature. The more extensive clone libraries from HS3i, however, failed to detect any cyanobacteria sequences and since the prominent polyenoic compound was 18 : 2ω6, like that of the service water, the polyenoics probably represent fungi. It is also possible that it may represent a carry over from the neutral lipids in the case of the Carbon Leader samples.

The microbial enrichments for HS3i, like those for most of the Carbon Leader samples, yielded mesophilic aerobic and nitrate, Fe(III)- and sulphate-reducing anaerobes and possibly fermenters. The only thermophiles detected were fermenters and Fe(III)- and MnO_2-reducing bacteria (Table 4). Thermophilic sulphate reduction was not detected in the enrichments of HS3i or in the $^{35}SO_4$ autoradiographic experiment, although one spot of $^{35}SO_4$ reducing activity was seen for HS4. Given that the terminally branched and mid-chain branched saturates were below the detection limit, with the exception of the parings, it is likely that the anaerobic constituents in the Carbon Leader are greatly outnumbered by their aerobic counterparts, explaining their absence in the clone libraries. The dominance of aerobic mesophiles in the enrichments and the clone libraries appears inconsistent with the anaerobic nature of the pore fluids, the submicron pore throat size and the 48°C formation temperature, unless they are interpreted as mining contaminants concentrated within mining-induced microfractures.

In contrast to the Carbon Leader, the quartzite block samples yielded less positive enrichments, RT aerobic heterotrophs, fermenters, MnO_2 and sulphate reducers and 60°C fermenters and sulphate reducers (HS2i in Table 4). The 60°C $^{35}SO_4$ autoradiography also did detected sulphate reduction at a number of points in the rock (Fig. 4A). Unlike the PLFA profiles of the Carbon Leader samples, that of HS2i contained less polyenoics and more terminally branched and mid-branched saturates including the biomarker for *Desulfobacter* (10me16:0). The 10me16:0 concentration corresponds to ~10^3 cells g^{-1}. No DNA was extracted from HS2i, but its PLFA analysis is very similar to that of the quartzite sample collected at Mponeng (Onstott *et al.*, 1997). The total PLFA for this quartzite was 2 pmole g^{-1}, with 82% normal saturates, 15% monoenoics, 2% mid-branched

saturates, 1% terminally branched saturates and only 2% polyenoics. DNA extraction, amplification, cloning and sequencing of this sample yielded two clones with 16S rDNA sequences similar to *Desulfobulbus* and *Desulforhopalus*.

The Br/CL of the fracture water (U Drill W and Final Drill in Table 2A) indicates that it is a 50:50 mixture of service water and pore water. Its NO_3 concentrations were less and SO_4 were more than those of the drilling water. The 10me16:0, which was absent in the drill water, was present in the fracture water at a concentration corresponding to ~10^3 cells ml^{-1}. Surprising is the polyenoic concentration which is 10–100× greater than that of the drilling water.

Microbial contamination of the rock and fracture water samples

Because the service water and air were expected to contain microbial constituents that originated not only from the surface, but also from the rock and water-bearing fractures, determining which species are contaminants and which are indigenous microorganisms that are released from the rock into the service water or air requires the use of both chemical and physical tracers. The Rhodamine WT permits the percentage volume of service water (whether carrying service water or air borne microorganisms) transferred into the rock and the fluorescent microspheres permits the percentage of particles adsorbed by the rock to be estimated without knowing the total volume of service water that flowed through the rock by using the following formula (Onstott *et al.*, 1998b):

$$\%\text{Contamination} = 100 \times [(T_s/T_c) \times (A_c/A_s - 1)]/[1 - T_s/T_c] \qquad (1)$$

where T_c is the measured tracer concentration in the service water, T_s is the measured tracer concentration in the rock sample, A_c is the microbial concentration in the service water and A_s is the microbial concentration in the rock.

The parings yielded T_s/T_c values of 10^{-3}–10^{-2}, whereas, the internal chunks, HS3i, HS2i, and 3–3CLi, all yielded T_s/T_c values <10^{-4} for both tracers (Table 1), or a >10× reduction in contamination from parings to internal chunk. Core parings record much greater levels of contamination with T_s/T_c values of 0.8–0.9 for the Rhodamine WT and 0.02–0.002 for the microspheres. Only the parings of the cores could be analysed for tracers as the internal chunk, E5 46/48 RC 0.7i, was only large enough for PLFA analyses and enrichments. The PLFA for E5 46/48 RC 0.7i, however, was 10× less than that of the parings and the PLFA was composed of normal saturates, monoenoics and 10× less polyenoics than the parings.

The bacterial biomass concentration in the stope water, 10^4 cells ml^{-1}, was comparable to that for the Carbon Leader, 10^{4-5} cells g^{-1}. Based upon these values, $A_c/A_s \sim 1$ and equation 1 indicate that <1% of the bacterial biomass in the stope face, block or core samples could be direct contaminants from sampling. This result is consistent with the 16S rDNA results of the clone libraries.

The dominance of mesophiles in the enrichment data of the Carbon Leader samples and the similarities between the PLFA and in the dominant phylum of the Carbon Leader samples with those of the service water, however, suggest microbial mining contaminants have penetrated these samples along mining-induced micro-fractures prior to mining of the rocks. Thermal modelling of the rock temperature as a function of mining rate indicates that the rock is at a temperature of ~30–35°C for 10–14 days before being removed. The cooling combined with O_2 diffusion along the mining-induced fractures means that mesophilic aerobes and fungi may have sufficient time to accumulate along the microfractures even if they cannot penetrate the narrow pore throats of the rock matrix.

If the T-RFLP data were treated as a spectrograph (ignoring the bias introduced by PCR amplification) then the relative area of each T-RFLP peak multiplied by the total PLFA concentration provides an estimate of the biomass of each ribotype in the service water versus the Carbon Leader. If the peaks unique to the Carbon Leader T-RFLP represent indigenous microorganisms, then their estimated biomass according to this is ~10^2 cells g^{-1}.

The 60°C enrichment and $^{35}SO_4$ autoradiography data for the quartzite block sample and the dissimilarity between its PLFA data (HS2i in Fig. 6) and that of the service water suggest that it is less contaminated and that indigenous SRB's exist within the quartzite at a concentration of ~10^3 cells g^{-1}. This biomass concentration is much less than the ~10^{4-5} cells g^{-1} determined for subsurface cores from Taylorsville and Piceance basins. If these SRB's have resided within the quartzite for the maximum allowable time of ~80 Myr., then a mechanism for sustaining the high pore water sulphate concentrations is required and this mechanism may be oxidation of sulphide by radiolytically produced O_2 and H_2O_2.

The internal fragments of the core samples also exhibited less evidence of contamination based upon the PLFA analyses (E5 46/48 RC 0.7i, 0.7p and 0.8p in Fig. 6). Future rock sampling for microbial analyses should focus on coring at least a few metres behind tunnel faces to avoid the intense fracturing which appears to create conditions for bacterial and fungal contamination and to verify that pore water and rock chemistry is not an artifact of O_2 diffusion through microfractures. Eukaryotic 18S rDNA probes should be used to determine whether polyenoic fatty acids do represent fungal contaminants. Finally, ther-

mophilic enrichments and autoradiography need to be employed to filter out mesophilic contaminants before DNA analyses.

Experimental procedures

Geochemical analysis

To insure that reduced solid and aqueous species were not inadvertently oxidized, the samples were kept frozen in the sterile Whirlpak bags inside the mason jars with N_2/H_2 atmospheres until they were transferred to the anaerobic glove bag. The pore water chemistry of the Carbon Leader and quartzite block samples (HS2 and 3 in Table 2) were determined by degassed, D.I. water extraction of 10 g fragments for 2 weeks in the anaerobic glove bag.

The solid phase Mn, Fe, S, Al, As and U species in HS3, HS2 and a pyrite standard were sequentially extracted by adapting the procedures of La Force and Fendorf (2000), Mehra and Jackson (1960) and Chao and Sanzolone (1977). Each sample (1 g) was reduced to powder within the glove bag before transfer into 50 ml centrifuge tubes. The aqueous species were first extracted with D.I. water (10 ml) for 1 h and then centrifuged at 2200 g for 5 min. The supernate was decanted into 15 ml test tubes. The exchangeable species present were extracted with 1 M $MgCl_2$ (10 ml) at pH 7 added to the residual wet powder and shaken for 1 h. The supernatant was decanted after the tube was centrifuged at 2200 g for 5 min. D.I. water (10 ml) was added to the residual powder, shaken, decanted and added to the extract.

To remove the species associated with the organic phase, concentrated Na hypochlorite (10 ml) was added to the residual powder and transferred to a 140 ml serum vial that was then crimped sealed. The serum vial was heated in an oven at 95°C for 30 min. The supernatant was decanted in the glove bag and this extraction repeated two more times. The residual powder was then removed from the glove bag.

To extract the ions associated with hydroxide and oxide phases (with the exception of magnetite) 0.11 M $NaHCO_3$ and 0.89 M Na citrate solution (45 ml) preheated to 80°C was added to the residual powder and the suspension transferred to 125 ml flasks. These were then placed in an oven at 80°C. Two grams of Na dithionite was added and the flask was shaken after 5–10 min to dissolve the Na dithionite. The suspension was heated for 1 h at 80°C, after which it was centrifuged at 2200 g for 5 min, the supernate decanted and the residual powder rinsed with D.I. water (10 ml).

To remove the species associated with sulphide, $KClO_3$ (1 g) and concentrated HCl (10 ml) was added to the residual powder. After 30 min at RT D.I. water (10 ml) was added, the suspension centrifuged at 2200 g for 5 min and the supernate decanted. To obtain the Fe species present in well-crystallized silicate and magnetite species 4 N HNO_3 (10 ml) was added to the residual powder and heated to a slow boil on a hot plate for 20 min.

The total Al, Mn, Fe, S, As and U of the extracts were determined by ICP-AES. The S was not measured for the Na dithionite extraction. The S of the subsequent $KClO_3$ extract may be overestimated due to residual Na dithionite not

removed by the D.I. rinse, but this is negligible considering the total Fe and S for the pyrite standard were slightly above 100%.

Enrichment procedures

The 140 ml serum vials of rock chips and service water were shaken in phosphate buffer and the suspension was removed with sterile syringe and used to inoculate several different types of media. MPN analyses were performed on select samples by using varying volumes of the suspension and the cell concentration calculated in terms of grams of extracted rock fragments. Most of the enrichments were incubated at RT and 60°C. The media were examined for signs of growth by colour change and/or increase in turbidity on site (3–6 weeks) and verified later by microscopy. The following media were utilized: *Thiobacillus denitrificans* media (T. denitrif. in Table 3), hydrogenotrophic medium ($H_2 + O_2$ in Table 3), S° oxidizing media (So oxi. in Table 3), S° reducing media (S° red. in Table 3), aerobic *Sulfolobus* media (Aero. Sulf. in Table 3), anaerobic *Sulfolobus* media (Anaero. Sulf. in Table 3), aerobic heterotroph media (Aero. TYG in Table 3), fermentative media with nitrate (Anaero. TYG in Table 3), fermentative media without nitrate (Anaero. TYEG in Table 3), denitrifier media (NRB in Table 3), Fe(III) reducing media with hydrous ferric oxide, HFO, and bicarbonate buffer (HFO in Table 3), Fe(III)-NTA reducing media (Fe(III)-NTA in Table 3), dilute Fe(III)-NTA reducing media (Basal Fe(III)-NTA in Table 3, HFO reducing media with PIPES buffer (HFO PIPES in Table 3), Fe(III)-citrate reducing media (Fe(III)-citrate in Table 3, Mn(IV) reducing media (MnO_2 in Table 3), sulphate reducing media with a phosphate buffer (SRB in Table 3), sulphate reducing media with MOPS buffer (SRB/Meth. in Table 3) and CO_2 reducing media (H_2/CO_2 in Table 3).

The anaerobic media were dispensed and sealed in pressure tubes under an 80% N_2 and 20% CO_2 headspace and autoclaved at 121°C for 35 min. Ten ml H_2 was added as an additional electron donor to all of the anaerobic media with the exception of the anaerobic *Sulfolobus* media and some of the anaerobic TYEG media. When warranted NaCl was added to the media to raise the salinity to 1% (w/v).

PLFA analysis

Cellular fatty acid composition was analysed using the procedures described by White and Ringelberg (1998). After extracting the sample by a modified single-phase chloroform-methanol-phosphate buffer procedure. (Bligh and Dyer, 1959; White *et al.*, 1979) the total extractable lipid was fractionated on a silicic acid column using a microtechnique (Tunlid *et al.*, 1989). The polar lipid fraction was collected and transesterified into fatty acid methyl esters (FAMEs) by mild alkaline methanolysis for gas chromatography/mass spectrometry (GC/MS) analysis (Guckert *et al.*, 1985; White and Ringelberg, 1998). The identity of FAMEs was verified using GC/MS in comparison with standards (Matreya, Pleasant Gap, PA) using previously published GC/MS conditions (White and Ringelberg, 1998; Takai *et al.*, 2001b).

DNA analysis

DNA extraction from filters (e.g. service water and mine air samples) followed the procedures of Moser *et al.* (2003). DNA was extracted from rock samples using an adaptation of the method of Chandler *et al.*, 1997). Before processing the samples, a calibration was performed in which Gram-positive (*Bacillus subtilus*) and Gram-negative (*Shewanella oneidensis*) bacterial cells were added to Carbon Leader samples, ground on dry ice and subjected to varying lengths of bead beating. Carbon Leader material, even with 10 s of beating, sheared the bacterial DNA into <500–750 bp fragments (as estimated by agarose gel electrophoresis). In contrast, hand grinding alone liberated 1500 bp DNA fragments. All metal tools for rock processing were first cleaned with soapy water, rinsed in D.I. water, then rinsed in a 10% bleach solution, autoclaved and heated for 12 h at 500°C. All processing work was performed in a HEPA-filtered laminar flow hood fitted with a UV lamp. In preparation for sample processing, the hood environment was first exposed to UV for 2 h, then wiped down with a 10% bleach solution, and finally UV irradiated for an additional 30 min, during which an autoclaved plastic tray filled with dry ice was also exposed to the UV lamp.

Carbon Leader samples, 7–14 g, were first crushed on dry ice in a stainless steel tray using an autoclaved and ethanol flamed stainless dowel and a ball peen hammer. These fragments were then ground to a fine powder with a ceramic mortar and pestle, on dry ice. Ground samples were mixed into sterile, filtered DNA extraction buffer (200 mM Na_2HPO_4, 100 mM EDTA, 1% SDS, pH 8.0) at a ratio of 1 ml buffer per gram of rock. The slurries were then vortexed on high for 2 min, subjected to a freeze-thaw cycle (dry ice, 30 min/70°C water bath, 10 min), spun in a clinical centrifuge for 5 min and the supernate decanted and saved. A second extraction with the same buffer (but lacking SDS) was performed, and the supernate pooled. The pooled extract was dialysed overnight in 10 mM Tris, 0.1 mM EDTA, at pH 8.0 using a 10 000 MWCO Slide-A-Lyzer dialysis chamber (Pierce, Rockford, IL). For DNA recovery, 0.2 vol. 7.5 M NH_4OAc and 2.0 vol. 100% EtOH (−20°C) was added to the dialysate followed by overnight precipitation at −20°C. After centrifugation at 10 000 g for 40 min at 4°C the resulting (invisible) DNA pellet was washed with 70% EtOH, dried under vacuum and dissolved in 50 µl of D.I. water.

DNA concentrations were determined by measuring OD_{260} with a Beckman DU70 spectrophotometer. Concentrations were high for the service water samples, EDS1 = 585 and E5-46-SW2 = 454 µg ml^{-1}, and the air condensate sample, E5-46-Air 1394 µg ml^{-1}. The DNA extracted from the Carbon Leader samples, however, was below detection.

Bacterial and archaeal 16S rDNA (SSU rDNA) were amplified using the approach of Moser *et al.* (2003). For clone libraries, oligonucleotide primers, B27f (5′-AGAGTTTGATC MTGGCTCAG-3′) (bacteria-specific, Giovannoni, 1991) and 907r (5′-CCGTCAATTCMTTTRAGTTT-3′) (universal, Lane, 1991) were used. The same primers were employed for TRFLP analysis, but B27f was labelled with 5′- tetrachlorofluorescein (PE Applied Biosystems, Foster City, CA). Archaeal PCR was performed using 21f (DeLong, 1992) and Arch915r (Stahl and Amann, 1991) or universal 1492r (Lane, 1991) primers. Clone libraries and DNA sequencing were

performed for two service water samples, one air sample and two internal rock fragments using the procedure of Moser *et al.* (2003). Clone libraries comprised 24–100 representative clones were obtained for each DNA extract. For several samples, DNA extractions were performed on duplicate samples and clone libraries were constructed to verify reproducibility. T-RFLP analysis of community rDNA was performed to obtain a minimum estimate of bacterial diversity in these samples using the procedures of Moser *et al.* (2003).

Phylogenetic analysis of cloned sequences was performed on the first 450–500 bases that could be read with confidence using the on-line Sequence Match feature at the Ribosomal Database Project (RDP (Maidak *et al.*, 1999) II web site (http://rdp.cme.msu.edu./cgis/seq_match.cgi?su = SSU) to identify the 16S rRNA sequences in the RDP database that were most similar to the clone sequences. The clone sequences were then tentatively placed into groups, each of which consisted of sequences that were most closely related to the same sequences in the RDP databases and therefore were likely to represent single and distinct ribotypes. The clone sequences were then evaluated in the context of the secondary structure (Gutell, 1994) of the 16S rRNA molecule for *Escherichia coli* (Brosius *et al.*, 1979) and re-examined and edited as needed. The GenBank accession numbers for the fully evaluated and edited sequences are AF459055-459076 and AF486654-486799.

The sequences in each putative clone type were aligned to select comparison sequences from the RDP and GenBank/EMBL databases following the approach of Moser *et al.* (2003). Comparison sequences included those in both databases that were most similar to the clone sequences and selected less similar sequences for comparison or for use as outliers during phylogenetic analyses. In the case of clone sequences with very low similarity to all sequences in the databases, the comparison sequences also included representatives from all of the major divisions of Bacteria designated by the RDP. This was done as part of an effort to better define the phylogenetic positions of the clones within this large group of sequences. All sequences were aligned manually, while taking into consideration the secondary structure. The phylogenetic relatedness of the clones to previously described bacteria and environmental clones was determined by comparison of the results from the three different phylogenetic methods and by evaluation of bootstrap data. This analysis further split sequences within the same clone type into two or more distinct clone types. These clone types were kept if the distinctions between them were retained in trees produced by all three analytical approaches.

Acknowledgements

References

Atlas, R.M. (1993) *Handbook of Microbiological Media*. Boca Raton: CRC Press.

Bligh, E.G., and Dyer, W.J. (1959) A rapid method of total lipid extraction and purification. *Can Biochem Phys* **37:** 911–917.

Brosius, J., Palmer, M.L., Kennedy, P.J., and Noller, H.F. (1979) The complete nucleotide sequence of the ribosomal 16-S RNA from *Escherichia coli*. Experimental details and cistron heterogeneities. *European J Biochem* **100:** 399–410.

Chandler, D.P, Brockman, F.J., and Fredrickson, J.K. (1997) Effect of PCR template concentration on the composition and distribution of total community 16S rDNA clone libraries. *Mol Ecol* **6:** 475–482.

Chao, T.T., and Sanzolone, R.F. (1977) Chemical dissolution of sulfide minerals. *J Res, U S Geol Survey* **5:** 409–412.

Colwell, F.S. Onstott, T.C. Dilwiche, M.E. Chandler, D. Fredrickson, J.K. Yao, Q.-J. *et al.* (1997) Microorganisms from deep, high temperature, sandstones: constraints on microbial colonization. *FEMS Microbiol Rev* **20:** 425–435.

Colwell, F.S., Stormberg, G.J., Phelps, T.J., Birnbaum, S.A., McKinley, J., Rawson, S.A. *et al.* (1992) Innovative techniques for collection of saturated and unsaturated subsurface basalts and sediments for microbiological characterization. *J Microbiololg Meth* **15:** 279–292.

Colwell, F.S., Yao, Q.-J., Onstott, T.C., and Murphy, E. (2002) Microbiology of deep high temperature sedimentary environments. In *The Encyclopedia of Environmental Microbiology*. New York: John Wiley & Sons.

DeLong, E.F. (1992) Archaea in coastal marine environments. *Proc Natl Acad Sci USA* **89:** 5685–5689.

Felsenstein, J. (1985) Confidence limits on phylogenies: an approach using the bootstrap. *Evolution* **39:** 783–791.

Felsenstein, J. (1993) *phylip (Phylogeny Inference Package)*, Version 3.5c. Seattle: University of Washington.

Fitch, W.M., and Margoliash, E. (1967) Construction of phylogenetic trees. *Science* **155:** 279–284.

Fredrickson, J.K., and Phelps, T.J. (1997) Subsurface drilling and sampling. In *Manual of Environmental Microbiology*. Hurst, C.J., Knudsen, G.R., McInerney, M.J., Stetzenbach, L.D. and Water, M.V., (eds). Washington, D.C.: American Society for Microbiology Press, pp. 526–540.

Fredrickson, J.K., McKinley, J.P., Bjornstad, B.N., Long, P.E., Ringelberg, D.B., White, D.C. *et al.* (1997) Pore-size constraints on the activity and survival of subsurface bacteria

in a Late Cretaceous shale-sandstone sequence, North-western New Mexico. *Geomicrobiol J* **14:** 183–202.

Frimmel, H.E., Hallbauer, D.K., and Gartz, V.H. (1999) Gold mobilizing fluids in the Witwatersrand Basin: composition and possible sources. *Mineral Petrol* **66:** 55–81.

Gay, N.C., and Jager, A.J. (1986) The influence of geological features on problems of rock mechanics in Witwatersrand mines. In *Mineral Deposits of Southern Africa*. Anhaeusser, C.R and Marke, S., (eds). Johannesburg: Geological Society of South Africa, pp. 753–722.

Giovannoni, S.J. (1991) The polymerase chain reaction. In *Nucleic Acid Techniques in Bacterial Systematics*. Stackebrandt, E. and Goodfellow, M., (eds). Chichester, England: John Wiley and Sons, pp. 177–203.

Gray, G.J., Lawrence, S.R., Kenyon, K., and Cornford, C. (1998) Nature and origin of 'carbon' in the Archaean Witwatersrand Basin, South Africa. *J Geol Soc London* **155:** 39–59.

Guckert, J.B., Antworth, C.P., Nichols, P.D., and White, D.C. (1985) Phospholipid, ester-linked fatty acid profiles as reproducible assays for changes in prokaryotic community structure of estuarine sediments. *FEMS Microbiol Ecol* **31:** 147–158.

Gutell, R.R. (1994) Collection of small subunit (16S- and 16S-like) ribosomal RNA structures. *Nucleic Acids Res* **17:** 3502–3507.

Hoffman, B.A. (1992) Isolated reduction phenomena in red beds. A result of porewater radiolysis? In *Water–Rock Interaction. Proceeding 7th International Symposium on Water–Rock Interaction.* Haraka, Y.K. and Maest, A.S., (eds). Rotterdam: A.A. Balkema, pp. 503–506.

Jukes, T.H., and Cantor, C.R. (1969) Evolution of protein molecules. In *Mammalian Protein Metabolism.* Munro, H.N., (ed). New York: Academic Press, pp. 21–132.

Katsivela, E., Wray, V., Pieper, D.H., and Wittich, R.M. (1999) Initial reactions in the biodegradation of 1-chloro-4-nitrobenzene by a newly isolated bacterium, strain LW1. *Appl Environ Microbiol* **65:** 1405–1412.

Kieft, T.L., Kovacik, W.B., Ringelberg, D.B., White, D.C., Haldeman, D.L., Amy, P.S., and Hersman, L.E. (1997) Factors limiting to microbial growth and activity at a proposed high-level nuclear repository, Yucca Mountain, Nevada. *Appl Environ Microbiol* **63:** 3128–3133.

Kieft, T.L., Fredrickson, J.K., Onstott, T.C., Gorby, Y.A., Kostandarithes, H.M., Bailey, T.J. *et al.* (1999) Dissimilatory reduction of Fe (III) and other electron acceptors by a Thermus isolate. *Appl Environ Microbiol* **65:** 1214–1221.

Krumholz, L.R., McKinley, J.P., Ulrich, G.A., and Suflita, J.M. (1997) Confined subsurface microbial communities in Cretaceous rock. *Nature* **386:** 64–66.

La Force, M.J., and Fendorf, S. (2000) Solid-phase iron characterization during common selective sequential extractions. *Soil Sci Soc Am Journal* **64:** 1608–1615.

Lane, D.J. (1991) 16S/23S rRNA sequencing. In *Nucleic Acid Techniques in Bacterial Systematics.* Stackebrandt, E., and Goodfellow, M., (eds). Chichester, England: John Wiley and Sons Ltd, pp. 115–175.

Lehman, R.M., Colwell, F.S., Ringelberg, D.B., and White, D.C. (1995) Combined microbial community-level analyses for quality assurance of terrestrial subsurface cores. *J Microbiol Meth* **22:** 263–281.

Lippmann, J., Stute, M., Torgersen, T., Moser, D.P., Hall, J., Lin, L. *et al.* (2003) Dating ultra-deep mine waters with noble gases and ^{36}Cl, Witwatersrand Basin, South Africa. *Geochimica Cosmochimica Acta* in press.

Maidak, B.L., Cole, J.R., Parker, J. Garrity, G.M., Larsen, N., Li, B. *et al.* (1999) A new version of the RDP (Ribosomal Database Project). *Nucleic Acids Res* **27:** 171–173.

Mehra, O.P., and Jackson, M.L. (1960) Iron oxide removal from soils and clays by dithionite-citrate system buffered with sodium bicarbonate. *Seventh National Conference on Clays and Clay Minerals*, pp. 317–327.

Moser, D.P., and Nealson, K.H. (1996) Growth of the facultative anaerobe *Shewanella putrefaciens* by elemental sulfur reduction. *Appl Environ Microbiol* **62:** 2100–2105.

Moser, D.P., Onstott, T.C., Balkwill, D.L., Takai, K., Pfiffner, S.M., White, D.C. *et al.* (2003) Evolution of microbial community structure and geochemistry in an ultradeep South African gold mine borehole. *Geomicrobiol J* in press.

Myers, C.R., and Nealson, K.H. (1988) Bacterial manganese reduction and growth with manganese oxide as the sole electron acceptor. *Science* **240:** 1319–1321.

Omar, G., Onstott, T.C., and Hoek, J. (2003) The origin of deep subsurface microbial communities in the Witwatersrand Basin, South Africa as deduced from apatite fission track analyses. *Geofluids* **3:** 69–80.

Onstott, T.C., Tobin, K., Dong, H., DeFlaun, M.F., Fredrickson, J.K., Bailey, T. *et al.* (1997) The deep gold mines of South Africa: window into the subsurface biosphere. *SPIE 42nd Annual Mtg.* San Diego: SPIE, pp. 344–357.

Onstott, T.C., Phelps, T.J., Kieft, T., Colwell, F.S., Balkwill, D.L., Fredrickson, J.K., and Brockman, F.J. (1998a) A global perspective on the microbial abundance and activity in the deep subsurface. In *Enigmatic Microorganisms and Life in Extreme Environments*. Seckbach, J., (ed). Dordrecht: Kluwer Academic Publishers.

Onstott, T.C., Phelps, T.J., Colwell, F.S., Ringelberg, D., White, D.C., Boone, D.R. *et al.* (1998b) Observations pertaining to the origin and ecology of microorganisms recovered from the deep subsurface of Taylorsville Basin, Virginia. *Geomicrobiol J* **15:** 353–385.

Phelps, T.J., Fliermans, C.B., Garland, T.R., Pfiffner, S.M., and White, D.C. (1989) Recovery of deep subsurface sediments for microbiological studies. *J Microbiol Meth* **9:** 267–280.

Postgate, J.R. (1984) *The Sulphate-Reducing Bacteria*. Cambridge: Cambridge Press.

Robb, F.T. (1995) Thermophiles. In *Archaea, a Laboratory Manual*. Robb, F.T., (ed). Cold spring Harbor: Cold spring Harbor Laboratory Press, p. 172.

Russell, C.E. (1997) The collection of subsurface samples by mining. In *The Microbiology of the Terrestrial Deep Subsurface*. Amy, P.S and Haldeman, D.L., (eds). Boca Raton, Fl: CRC Press, pp. 45–59.

Stahl, D.A., and Amann, R. (1991) Development and application of nucleic acid probes in bacterial systematics. In *Nucleic Acid Techniques in Bacterial Systematics*. Stackebrandt, E and Goodfellow, M., (eds). Chichester, England: John Wiley and Sons Ltd, pp. 205–248.

Swanson, B.F. (1981) A simple correlation between permeabilities and mercury capillary pressures. *J Petrol Technol* December: 2488–2504.

Takai, K., Moser, D.P., DeFlaun, M.F., Onstott, T.C., and Fredrickson, J.K. (2001a) Archaeal diversity in waters from deep South African Gold mines. *Appl Environ Microbiol* **67:** 5750–5760.

Takai, K., Moser, D.P., Onstott, T.C., Speolstra, N., Pfiffner, S.M., Dohnalkova, A., and Fredrickson, J.K. (2001b) Alcaliphilus auruminutor Gen nov., sp. nov., an extremely alkaliphilic bacterium isolated from a deep South African gold mine. *Int J Syst Bacteriol* **51:** 1245–1256.

Tiedje, J.M. (1982) *Denitrification in Methods of Soil Analysis.* Page, A.L., (ed.). Madison, Wisconsin: ASA, pp. 1011–1026.

Tseng, H.-Y., Onstott, T.C., Burruss, R.C., and Miller, D.S. (1995) Constraints on the thermal history of Taylorsville Basin, Virginia, USA, from fluid-inclusion and fission-track analyses: implications for subsurface geomicrobiology experiments. *Chem Geol* **127:** 269–294.

Tunlid, A., Ringelberg, D.B., Phelps, T.J., Low, C., and White, D.C. (1989) Measurement of phospholipid fatty acids at picomolar concentrations in biofilms and deep subsurface sediments using gas chromatography and chemical ionization mass spectrometry. *J Microbiol Meth* **10:** 139–153.

Washburn, F.W. (1921) Note on a method of determining pore size in porous material. *Proc Natl Acad Sci USA* **7:** 115–116.

White, D.C., Davis, W.M., Nickels, J.S., King, J.D., and Bobbie, R.J. (1979) Determination of the sedimentary microbial biomass by extractable lipid phosphate. *Oecologia* **40:** 51–62.

White, D.C., and Ringelberg, D.B. (1998) Signature lipid biomarker analysis. In *Techniques in Microbial Ecology.* Burlage, R.S., Atlas, R., Stahl, D.A. Geesey, G and Sayler, G., (eds). New York: Oxford University Press.

Wolin, E.A., Wolin, M.J., and Wolfe, R.S. (1963) Formation of methane by bacterial extracts. *J Biol Chem* **238:** 2882–2886.

Zumberge, J.E., Sigleo, A.C., and Nagy, B. (1978) Molecular and elemental analyses of the carbonaceous matter in the gold and uranium bearing Vaal Reef carbon seams, Witwatersrand Sequence. *Minerals Sci Engineering* **10:** 223–246.